



EDGEWOOD CHEMICAL BIOLOGICAL CENTER

U.S. ARMY RESEARCH, DEVELOPMENT AND ENGINEERING COMMAND
Aberdeen Proving Ground, MD 21010-5424

ECBC-TR-957

METAL ION-CATALYZED ALCOHOLYSIS AS A STRATEGY FOR THE HIGH LOADING DESTRUCTION OF CHEMICAL WARFARE ORGANOPHOSPHORUS AGENTS

H. Dupont Durst

RESEARCH AND TECHNOLOGY DIRECTORATE

R. Stanley Brown
Alexei A. Neverov
Andrea Tamer

QUEEN'S UNIVERSITY
Kingston, Ontario, Canada K7L 3N6

November 2013



Approved for public release; distribution is unlimited.



Disclaimer

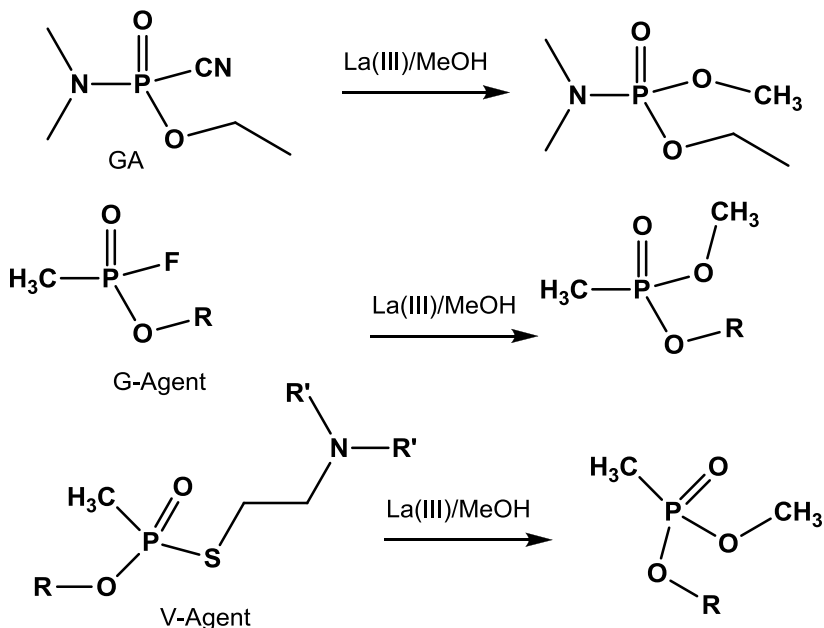
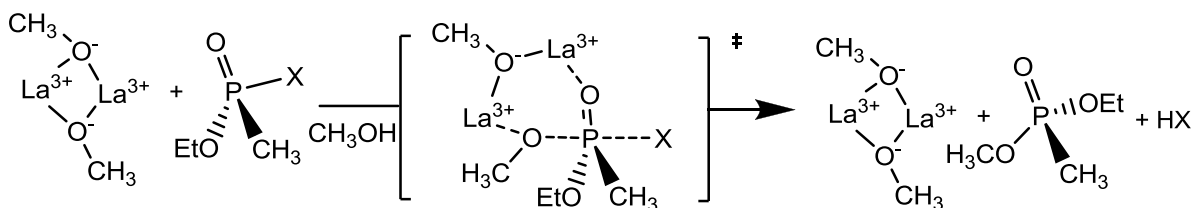
The findings in this report are not to be construed as an official Department of the Army position unless so designated by other authorizing documents.

REPORT DOCUMENTATION PAGE				Form Approved OMB No. 0704-0188	
Public reporting burden for this collection of information is estimated to average 1 hour per response, including the time for reviewing instructions, searching existing data sources, gathering and maintaining the data needed, and completing and reviewing this collection of information. Send comments regarding this burden estimate or any other aspect of this collection of information, including suggestions for reducing this burden to Department of Defense, Washington Headquarters Services, Directorate for Information Operations and Reports (0704-0188), 1215 Jefferson Davis Highway, Suite 1204, Arlington, VA 22202-4302. Respondents should be aware that notwithstanding any other provision of law, no person shall be subject to any penalty for failing to comply with a collection of information if it does not display a currently valid OMB control number. PLEASE DO NOT RETURN YOUR FORM TO THE ABOVE ADDRESS.					
1. REPORT DATE (DD-MM-YYYY) XX-11-2013		2. REPORT TYPE Final		3. DATES COVERED (From - To) Aug 2009 – Nov 2010	
4. TITLE AND SUBTITLE Metal Ion-Catalyzed Alcoholysis as a Strategy for the High Loading Destruction of Chemical Warfare Organophosphorus Agents				5a. CONTRACT NUMBER DHS IAA No. HSHQDC-09-X-00543	
				5b. GRANT NUMBER	
				5c. PROGRAM ELEMENT NUMBER	
6. AUTHOR(S) Durst, H. Dupont (ECBC); Brown, R. Stanley; Neverov, Alexei A.; and Tamer, Andrea (Queen's University)				5d. PROJECT NUMBER	
				5e. TASK NUMBER	
				5f. WORK UNIT NUMBER	
7. PERFORMING ORGANIZATION NAME(S) AND ADDRESS(ES) Director, U.S. Army Edgewood Chemical Biological Center, ATTN: RDCB-DRC-C, Aberdeen Proving Ground, MD 21010-5424 Department of Chemistry, Chernoff Hall, 90 Bader Lane, Queen's University, Kingston, Ontario, Canada K7L 3N6				8. PERFORMING ORGANIZATION REPORT NUMBER ECBC-TR-957	
9. SPONSORING / MONITORING AGENCY NAME(S) AND ADDRESS(ES) U.S. Department of Homeland Security, ATTN: Homeland Security Advanced Research Projects Agency, Washington, DC 20528-0001				10. SPONSOR/MONITOR'S ACRONYM(S) HSARPA	
				11. SPONSOR/MONITOR'S REPORT NUMBER(S)	
12. DISTRIBUTION / AVAILABILITY STATEMENT Approved for public release; distribution is unlimited.					
13. SUPPLEMENTARY NOTES					
14. ABSTRACT-LIMIT 200 WORDS Metal-catalyzed alcoholysis has proven to be an effective strategy for the rapid transformation of neutral reactive organophosphate esters of the phosphate, phosphonate, phosphorothioate, and phosphonothioate classes. This chemistry, using La^{3+} (^-OMe)/Methanol as catalyst/solvent, applied to the V and G classes of chemical warfare agents, demonstrated extremely rapid transformation to low toxicity esters with load factors of ~30% for non-fluoride-releasing agents. Variation of the alcohol solvent is tolerated. Variations of the metal catalyst provide potential redress to the fluoride inhibition of the G agent class. These observations indicate that formulations based on mixed alcohol solvents combined with optimized metal catalysts for use in field decontamination, civilian security, and infrastructure scenarios provide a pathway for "tuning" the reaction media while retaining extremely rapid destruction kinetics.					
15. SUBJECT TERMS Metal ion-catalyzed alcoholysis G and V nerve agents Pesticide Decontamination Chemical weapon (CW) ^{31}P -NMR					
16. SECURITY CLASSIFICATION OF:			17. LIMITATION OF ABSTRACT UU	18. NUMBER OF PAGES 54	19a. NAME OF RESPONSIBLE PERSON Renu B. Rastogi
a. REPORT U	b. ABSTRACT U	c. THIS PAGE U			19b. TELEPHONE NUMBER (include area code) (410) 436-7545

Blank

EXECUTIVE SUMMARY

Metal-catalyzed alcoholysis has proven to be an effective strategy for the rapid transformation of neutral reactive organophosphates esters of the phosphate, phosphonate, phosphorothioate, and phosphonothioate classes. This chemistry, using La^{3+} (OMe)/methanol as catalyst/solvent applied to the V and G classes of chemical weapons agents, demonstrated extremely rapid transformation to low toxicity esters with load factors of $\sim 30\%$ for non-fluoride-releasing agents. Variation of the alcohol solvent indicated that ethanol and monoethylamine are equally effective in this system. Synthetic chemistry was developed to rapidly provide independent standards of the diester products for unambiguous product assignment. In addition, variations of the metal catalyst provide potential redress to the fluoride inhibition of the G agent class. These observations indicate that formulations based on mixed alcohol solvents combined with optimized metal catalysts for use in field decontamination, civilian security, and infrastructure scenarios provide a pathway for “tuning” the reaction media while retaining extremely rapid destruction kinetics.



Graphical abstract: Overview of reaction mechanism with specific examples of products resulting from GA, fluoride-releasing G agent, and V agent.

Blank

PREFACE

The work described in this report was authorized under U.S. Department of Homeland Security Interagency Agreement contract no. HSHQDC-09-X-00543. The work was started in August 2009 and completed in November 2010.

The use of either trade or manufacturers' names in this report does not constitute an official endorsement of any commercial products. The report may not be cited for purposes of advertisement.

This report has been approved for public release.

Blank

CONTENTS

1.	INTRODUCTION	1
2.	ADVANTAGES OF METAL-CATALYZED ALCOHOLYSIS OVER HYDROLYSIS	1
3.	EFFECTS OF METAL ION CATALYSIS OF PHOSPHORYL TRANSFER IN METHANOL MEDIUM.....	3
4.	METHANOLYSIS OF PHOSPHOROTHIOATES, PHOSPHONATES, AND PHOSPHONOTHIOATES	7
5.	TRANSESTERIFICATION IN CWA DECONTAMINATION: BACKGROUND	10
5.1	Decontamination Solution 2 (DS2).....	10
5.2	Russian Reactive Decontaminant 4, Modified (RD4M).....	10
5.3	Mono-Ethylamine: U.S. Non-Stockpile Decontamination Solution.....	11
5.4	DS2, RD4M, and Mono-Ethanolamine: Advantages and Disadvantages	12
6.	EXPERIMENTAL METHODS.....	12
6.1	Simulant for G Agents Developed.....	12
6.2	Synthesis of Product Standards.....	14
6.3	Synthesis of Model EA 2192 Compounds.....	15
6.4	Ethanolamine/La ³⁺ -Mediated Decomposition of Phosphonate Substrates	16
6.4.1	Materials	16
6.4.2	Kinetics Study	16
6.5	CWA Experimental Design	17
6.5.1	Reaction Criteria	17
6.5.2	“Force-to-Fail” Criteria.....	17
6.5.3	Experimental Design.....	17
7.	RESULTS	20
7.1	Hydrolysis versus Transesterification: The EA 2192 Problem.....	20
7.2	Effect of Leaving Group on Reactivity of Model Compounds 11 and Prediction of EA 2192 Reactivity	22
7.3	Results for Ethanolamine/La ³⁺ -Mediated Decomposition of Phosphonate Substrates.....	23
7.4	Destruction of CWAs Using Force-to-Fail Criteria.....	26
7.5	TNO Agent Results.....	27
7.6	Agent Testing at Research Institute of Hygiene, Occupational Pathology, and Human Ecology (RIHOPHE)	28

8.	DISCUSSION	28
8.1	Destruction Efficiency of System 4	28
8.2	Alternative Solvents	29
8.3	Effects of Water on Reactivity	29
8.4	Simulant Reactivity	29
8.5	Production and Decomposition of EA 2192	30
8.6	Low-Level Residual Agent Concentration	30
9.	CONCLUSIONS	30
	LITERATURE CITED	31
	ACRONYMS AND ABBREVIATIONS	37

FIGURES

1. Plot of k_{obs} versus $[\text{La}(\text{OTf})_3]$ for the La^{3+} -catalyzed methanolysis of paraoxon **2** ($2.04 \times 10^{-5} \text{ mol dm}^{-3}$) at 25°C for ^spH values of 8.96 (■), 8.23 (○), and 7.724
2. Plot of $\log k_2$ versus ^spH for La^{3+} -catalyzed methanolysis of paraoxon **2** at 25°C 4
3. Plot of the predicted k_2^{obs} versus ^spH rate profile for La^{3+} -catalyzed methanolysis of paraoxon **2** (solid line) based on the kinetics contributions of (left to right), $\text{La}^{3+}_2(\text{OCH}_3)_1$, $\text{La}^{3+}_2(\text{OCH}_3)_2$, $\text{La}^{3+}_2(\text{OCH}_3)_3$, and $\text{La}^{3+}_2(\text{OCH}_3)_4$ computed from the $k_2^{2:1}$, $k_2^{2:2}$, $k_2^{2:3}$, and $k_2^{2:4}$ rate constants (Table 1) and their speciation as a function of ^spH 5
4. Brønsted plots for $\log k_2^{\text{catalyst}}$ versus $^s\text{pK}_a$ of aryl thiol with $(\text{La}^{3+}(\text{OCH}_3))_2$ (●), $4:\text{Zn}^{2+}(\text{OCH}_3)$ (▲), and OCH_3 (◆)9
5. Data example: GA reaction using System 4 (S4) from Queen's University19
6. Plot of pseudo-first-order rate constant for the methanolysis of **11a** ($1 \times 10^{-4} \text{ M}$) versus $[\text{La}(\text{OTf})_3]$ at $25.0 \pm 0.1^\circ\text{C}$ and a ^spH of 8.4 (in 0.04 M *N*-ethylmorpholine buffer)21
7. Plot of pseudo-first-order rate constant for the methanolysis of **11a** ($1 \times 10^{-4} \text{ M}$) versus $[\text{La}(\text{OTf})_3]$ at $25.0 \pm 0.1^\circ\text{C}$ and a ^spH of 11.7 (in 0.04 M triethylamine buffer)21
8. Brønsted plots for the La^{3+} -catalyzed methanolysis of EA 2192 analogues **11** (solid line) determined at ^spH of 11.7 and temperature of $25.0 \pm 0.1^\circ\text{C}$, where $\log k_{\text{cat}}^{8.4} = (4.02 \pm 0.36) - (0.69 \pm 0.03)^s\text{pK}_a^{\text{HSAr}}$, $r^2 = 0.99$; and (dashed line) determined at ^spH of 8.4 and temperature of $25.0 \pm 0.1^\circ\text{C}$, where $\log k_{\text{cat}}^{8.4} = (3.79 \pm 0.35) - (0.52 \pm 0.03)^s\text{pK}_a^{\text{HSAr}}$, $r^2 = 0.99$23

TABLES

1.	Computed Second-Order Rate Constants ($k_2^{2:n}$) for the $(\text{La}^{3+})_2(\text{OCH}_3)_n$ -Catalyzed Methanolysis of Paraoxon 2 Obtained through Fits of k_2^{obs} at Each ^spH to Eq 1	6
2.	Activation Parameters for the Base- and La^{3+} -Catalyzed Methanolysis of Dimethyl <i>p</i> -Nitrophenyl Phosphate (3) and Dimethyl Phenyl Phosphate (4).....	7
3.	Expected $t^{1/2}$ Times for the Methanolysis of Organophosphates 5 , 6 , and 7 Catalyzed by a 1 mmol dm ⁻³ Solution of Various Metal Ion Complexes at 25 °C	8
4.	^spH Dependence of the Second-Order Rate Constant for the Reaction of 11b with $\text{La}^{3+}(\text{CH}_3\text{O}^-)_m(k_1)$ and Pseudo-First-Order Rate Constant for Methanolysis of $(\text{La}^{3+})_2\text{:2:}(\text{CH}_3\text{O}^-)_n(k_{\text{cat}})$ at 25.0 ± 0.1 °C	22
5.	Concentration Dependence of Various La-Based Catalysts in EA toward Solvolysis of <i>p</i> -Nitrophenyl Ethyl Methylphosphonate (0.02 mM) at 25 °C	23
6.	Concentration Dependence of Various La-Based Catalysts in EA/Ethanol Mixture (70/30% v/v) toward Solvolysis of <i>p</i> -Nitrophenyl Ethyl Methylphosphonate (0.02 mM) at 25 °C	24
7.	Concentration Dependence of Various La-Based Catalysts in EA/Methanol Mixture (70/30% v/v) toward Solvolysis of <i>p</i> -Nitrophenyl Ethyl Methylphosphonate (0.02 mM) at 25 °C	24
8.	Effect of Extraneous Water Added to the 5 mM Solution of $\text{La}(\text{OTf})_3$ in EA, EA/Ethanol Mixture (70/30% v/v), and EA/Methanol Mixture (70/30% v/v) on the Solvolysis Rate of <i>p</i> -Nitrophenyl Ethyl Methylphosphonate (0.02 mM) at 25 °C.....	24
9.	Effects of Fluoride Anion Addition to the 5 mM $\text{La}(\text{OTf})_3$ Solution in EA, EA/Ethanol Mixture (70/30% v/v), and EA/Methanol Mixture (70/30% v/v) on the Solvolysis Rate of <i>p</i> -Nitrophenyl Ethyl Methylphosphonate (0.02 mM) at 25 °C.....	24
10.	Effects of Extraneous Water Added to the 5 mM $\text{Sm}(\text{OTf})_3$ Solution in EA and EA/Ethanol Mixture (70/30% v/v) on the Solvolysis Rate of <i>p</i> -Nitrophenyl Ethyl Methylphosphonate (0.02 mM) at 25 °C	25
11.	Effects of $\text{La}(\text{OTf})_3$ Aging in the Presence of 20% (v/v) Water on the Rate Constant for Reaction with <i>p</i> -Nitrophenyl Ethyl Methylphosphonate in EA and EA/Ethanol Mixture (70/30% v/v) at 25 °C	25

12.	Effects of $\text{Sm}(\text{OTf})_3$ Aging in the Presence of 20% (v/v) Water on the Rate Constant for the Reaction with <i>p</i> -Nitrophenyl Ethyl Methylphosphonate in EA and EA/Ethanol Mixture (70/30% v/v) at 25 °C.....	25
13.	Effects of Extraneous Water Added to the 100 mM $\text{La}(\text{OTf})_3$ Solution in EA and EA/Ethanol Mixture (70/30% v/v) on the Paraoxon (0.02 mM) Solvolysis Rate at 25 °C	25
14.	Effects of Extraneous Water Added to the 50 mM $\text{La}(\text{OTf})_3$ Solution in EA and EA/Ethanol Mixture (70/30% v/v) on the Paraoxon (0.02 mM) Solvolysis Rate at 25 °C	26
15.	Effects of Extraneous Water Added to the 30 mM $\text{La}(\text{OTf})_3$ Solution in EA and EA/Ethanol Mixture (70%/30% v/v) on the Paraoxon (0.02 mM) Solvolysis Rate at 25 °C	26
16.	Effects of Extraneous Water Added to the 50 mM $\text{Sm}(\text{OTf})_3$ Solution in EA and EA/Ethanol Mixture (70%/30% v/v) on the Paraoxon (0.02 mM) Solvolysis Rate	26
17.	Catalytic Systems Formulated and Tested for Efficacy in Decomposing OP CWAs	27
18.	Decontamination Efficiency of Decontamination System against GA, GD, VX, and HD on CARC Panels.....	28

STRUCTURES

1.	General representation of reactive phosphate diesters and monoesters showing the type of leaving group (LG) associated with these structures	3
2.	Paraoxon	3
3.	Dimethyl <i>p</i> -nitrophenyl phosphate	7
4.	Dimethyl phenyl phosphate	7
5.	Ethyl aryl methylphosphonate	8
6.	Dimethyl aryl phosphorothioate	8
7.	Ethyl aryl methylphosphonothiate	8
8.	$\text{Zn}^{2+}(\text{OCH}_3^-)$ and $\text{Cu}^{2+}(\text{OCH}_3^-)$ complex.....	8
9.	<i>S</i> -aryl methylphosphonothioates	8
10.	U.S. VX (USVX): <i>O</i> -ethyl- <i>S</i> -(2-diisopropylaminoethyl) methylphosphonothioate	9
11.	Model EA 2192 compounds with various leaving groups.....	20

Blank

METAL ION-CATALYZED ALCOHOLYSIS AS A STRATEGY FOR THE HIGH LOADING DESTRUCTION OF CHEMICAL WARFARE ORGANOPHOSPHORUS AGENTS

1. INTRODUCTION

Activated organophosphate, phosphinate, and phosphonate esters are potent acetylcholinesterase inhibitors that are used as animal and crop protectants and chemical warfare agents (CWAs). Whether these inhibitors are used as pesticides or CWAs, all act in the same way by inhibiting an enzyme (a cholinesterase), thereby interfering with normal neurotransmission and ultimately leading to respiratory failure and death. The use of organophosphorus (OP) pesticides such as malathion, diazinon, cygon (dimethoate), and other easily available materials is widespread, and most of these can be purchased in an unrestricted fashion. Recent estimates by the U.S. Environmental Protection Agency indicate that in the United States, 73 million pounds of the active ingredients for these inhibitors are used annually, accounting for 70% of all insecticides used for agriculture, in homes and gardens, and for government purposes. Estimates of quantities used throughout the world are about 10 times this amount, or 365,000 tons per year. Despite the beneficial uses of these inhibitors, increasing concern exists regarding soil and water contamination arising from spills and improper applications. At the same time, needs for pesticides are increasing to sustain worldwide food demand, so it is highly unlikely that use of these inhibitors will be eliminated in the near future.

Recent geopolitical events have cast much attention on OP CWAs. Developed and widely stockpiled as defensive measures by several countries after World War II, these materials have no present legitimate purpose other than as deterrents to First Strike use by potential belligerents. Concerns are increasing that these materials, whether home-synthesized or pilfered from stockpiled or found sources, could become preferred weapons of terrorist organizations. In an effort to rid the world of these materials, the 1992 Chemical Weapons Convention Treaty¹ required total destruction of scheduled chemical weapons (CWs) stockpiles by the signatory nations (188 nations as of April 2009, representing more than 95% of the world population) by 2012.

Given the abundance and lethality of OP CWs and the increasing possibilities of terrorist activities, considerable research was and is being performed to create methods of facilitating the controlled decomposition of OP materials.²⁻⁶ Although good methods exist for the decomposition of many of these materials, many have deficiencies, and no single technique is appropriate for all types of CWs; therefore, an urgent need exists for new, fast, and effective decontamination methodologies.

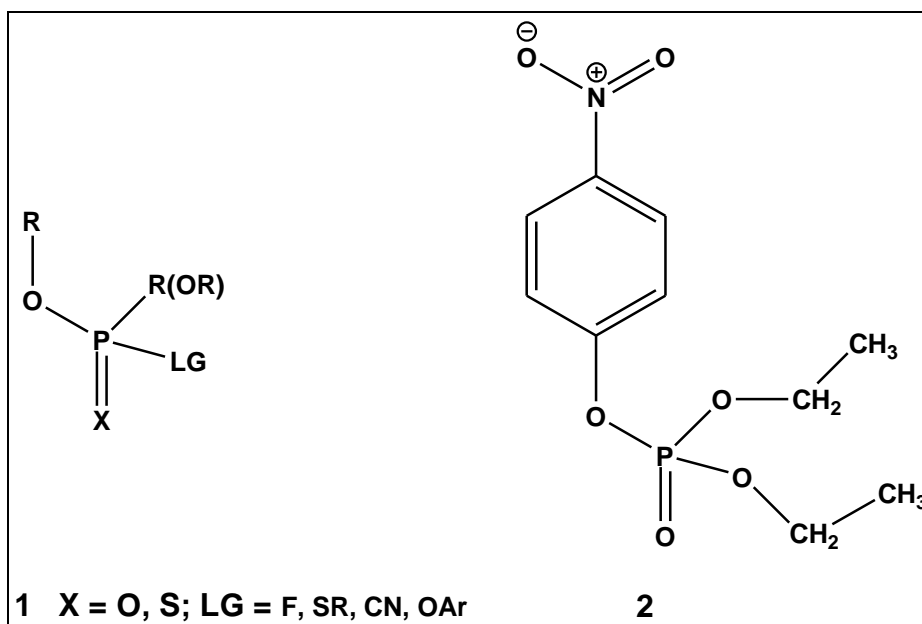
2. ADVANTAGES OF METAL-CATALYZED ALCOHOLYSIS OVER HYDROLYSIS

Metal ion-catalyzed alcoholysis reactions for inactivating reactive OP esters have been studied for many years.⁷⁻⁹ These are relatively well-understood processes in which the reactions typically involve catalytically active $M^{x+}(OR)$ species with the metal ion playing several roles, including:

- (1) Decreasing the pKa of the metal associated HOR so that an $M^{x+}(-OR)$ can be formed at, or near, neutral pH;
- (2) A bifunctional role where the $M^{x+}(-OR)$ acts as a Lewis acid coordinating transiently to the P=O group, allowing a subsequent intramolecular delivery of the coordinated alkoxide; and
- (3) Possibly promoting an accelerated breakdown of any intermediates through coordination of the leaving group (particularly a poor one) to the metal ion.

Water is required as a reagent for hydrolytic processes; however, there are significant disadvantages associated with using it as a reaction medium for metal-catalyzed reactions. Although the $M^{x+}(-OH)$ species are catalytically active, they generally form oligomeric and polymeric gels or precipitates that are poorly soluble in aqueous media, which complicates mechanistic analyses, particularly at higher pH. By contrast, their alkoxide analogs ($M^{x+}(-OR)$) are soluble, even at relatively high concentrations in alcohol at high pH; therefore, detailed studies of metal ion-catalyzed alcoholysis (MICA) reactions of carboxylate and phosphate esters are possible.⁵ Perhaps more importantly, M^{x+} hydroxides in water are not particularly reactive intermolecular catalysts for phosphoryl or acyl transfer reactions, and with rare exception, they are generally less reactive than free hydroxide for these processes. This might be expected for a system where stabilizing a coordinated hydroxide by binding it to an electropositive metal ion should decrease its basicity and nucleophilicity. In such cases, the catalytic role of the metal ion is limited to providing a sufficient concentration of nucleophile (coordinated hydroxide) at lower pH values. However, we have found that M^{x+} -coordinated alkoxides in alcohol solvents are good nucleophiles toward neutral phosphates and carboxylate esters with activities that are generally much higher than those for free alkoxide. Yang has reported⁵ that there is a synergistic role between low-polarity, reduced-dielectric constant alcohol solvents and metal-coordinated alkoxides that leads to high reactivity of these systems. This probably includes several factors such as increasing the transient ion-dipole binding of the metal complex and substrate and decreasing the activation energy for reaction of the bound substrate-metal complex through a lower-polarity-solvent effect that favors transition states in which charge is dispersed relative to ground state.

Although phosphate triesters are not naturally occurring molecules and, therefore, have no known natural biological function, nature produces a class of phosphotriesterase (PTE) enzymes that are very effective at destroying neutral OP pesticides and thereby protecting organisms from OP poisoning. The two most studied PTEs, from *Agrobacterium radiobacter* and *Pseudomonas diminuta*, are dinuclear Zn(II) enzymes that have nearly 90% amino acid homology and conserve all the metal-binding ligands.¹⁰ Although it is not exactly established, the mechanism of action for these enzymes has been discussed as involving intramolecular delivery of a Zn(II)-coordinated hydroxide (possibly one bridged between the two Zn(II) ions) to a neutral phosphate ester substrate that is activated by P=O-coordination to the second Zn(II) ion.^{11,12} This sort of dinuclear core is characteristic of other enzymes that mediate hydrolytic cleavage of phosphate diesters¹³⁻¹⁸ and monoesters¹⁹ and gives the *P. diminuta* bacterium the ability to hydrolytically decompose paraoxon **2**, its preferred substrate, with a rate constant (k_{cat}) near the diffusion limit, $k_{cat}/K_m \sim 10^8 \text{ mol}^{-1} \text{ dm}^3 \text{ s}^{-1}$ (where K_m is the Michaelis constant).²⁰ Importantly, PTE enzymes also react with OP chemical weapons, which suggests that enzyme-based systems or enzymes mimicking these detoxifying systems might be useful for decontamination.



Structure 1. General representation of reactive phosphate diesters and monoesters showing the type of leaving group (LG) associated with these structures.
 Structure 2. Paraoxon (CAS no. 311-45-5).

Our strategy toward developing an artificial phosphotriesterase was based on the idea of a metal-coordinated nucleophile in a reduced-polarity medium having a greater interaction with substrate and greater reactivity than is possible in water. Cleland et al.²¹ have suggested that “enzyme active sites are non-aqueous, and the effective dielectric constants resemble those in organic solvents rather than that in water”. Given that the dielectric constants of water, methanol, and ethanol are 78, 32.7, and 24.6, the light alcohols were chosen as the medium for mimicking the reduced-polarity environment that is assumed to exist for the PTE enzymes.

3. EFFECTS OF METAL ION CATALYSIS OF PHOSPHORYL TRANSFER IN METHANOL MEDIUM

Our original experiments investigating MICA of phosphate esters involved the methanolysis of the pesticide paraoxon promoted by La³⁺ in methanol.²² As shown in Figure 1, plots of the observed first-order rate constant (k_{obs}) versus lanthanum trifluoromethanesulfonate (La(OTf)₃) concentration at three different pH values in methanol (designated as ^spH)^{5,12} are linear at higher La³⁺ concentrations with an upward curvature at lower concentrations. The upward curvature of the plot at lower La³⁺ concentrations indicates that the reaction is second-order in La³⁺ concentration. The slopes of the linear sections of the graphs at higher La³⁺ concentrations are ^spH dependent and are defined as the observed second-order rate constants (k_2^{obs}) values for the (La³⁺)₂-catalyzed reaction. A plot is presented in Figure 2 of the log k_2^{obs} versus ^spH profile for the (La³⁺)₂-catalyzed reaction, which shows a distorted bell-shaped profile that plateaus between ^spH values of 8 and 10.5.

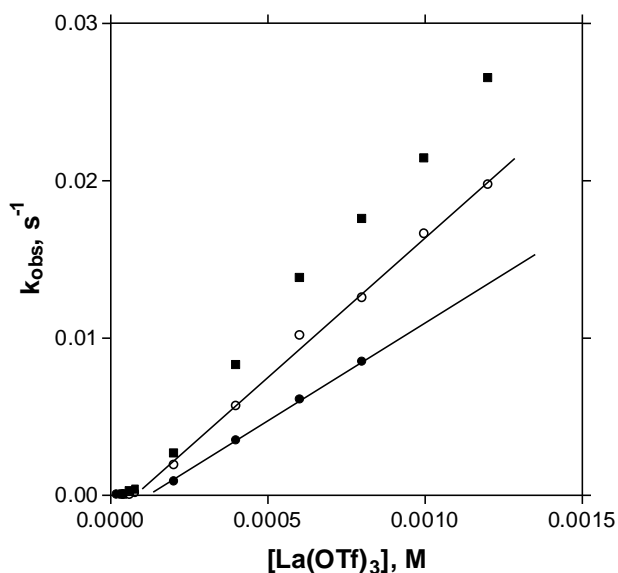


Figure 1. Plot of k_{obs} vs. $[\text{La}(\text{OTf})_3]$ for the La^{3+} -catalyzed methanolysis of paraoxon **2** ($2.04 \times 10^{-5} \text{ mol dm}^{-3}$) at 25°C for ^spH values of 8.96 (■), 8.23 (○), and 7.72. (Reproduced with permission from Tsang et al.²²)

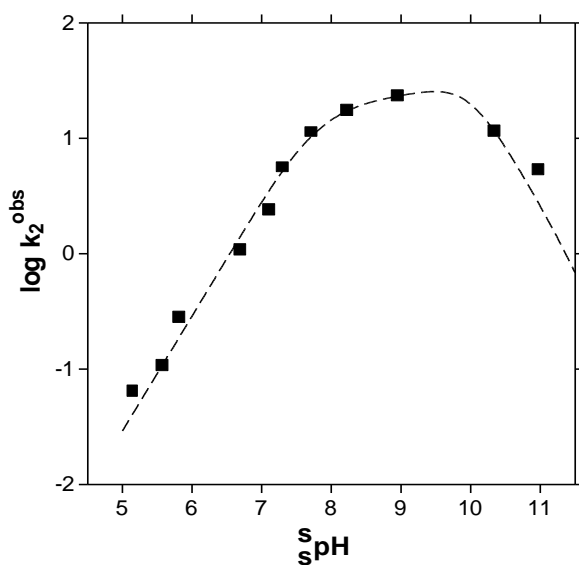


Figure 2. Plot of $\log k_2$ vs. ^spH for La^{3+} -catalyzed methanolysis of paraoxon **2** at 25°C . (Reproduced with permission from Tsang et al.²²)

The reactions in the plateau region are very fast, and it can be calculated from the k_2^{obs} values that at ^spH 8.3–8.4 (neutral ^spH in methanol), a 2 mol dm^{-3} solution of La^{3+} (1 mol dm^{-3} in $(\text{La}^{3+})_2$) has a half-life ($t_{1/2}$) time of 20 s for destruction of paraoxon. This corresponds to a 10^9 -fold acceleration relative to the background reaction under those conditions (the uncatalyzed $t_{1/2}$ is reported to be ~ 600 years at a near neutral ^spH of 8.3)¹². Further analysis

involving potentiometric titrations of La^{3+} in methanol^{7,23} indicated that the dimeric species responsible for catalysis had increasing numbers of associated methoxides at higher ^spH values (species represented as $(\text{La}^{3+})_2(\text{OCH}_3)_n$, where n assumes the values of 1–5). A detailed analysis of the data yielded the speciation diagram of $\text{La}^{3+}_2(\text{OCH}_3)_n$ complexes under the experimental conditions that are presented in Figure 3. These are shown together with the overlaid k_2^{obs} kinetics data to indicate that the dominant catalytically active species is $(\text{La}^{3+})_2(\text{OCH}_3)_2$ operating at a ^spH of ~ 9 .

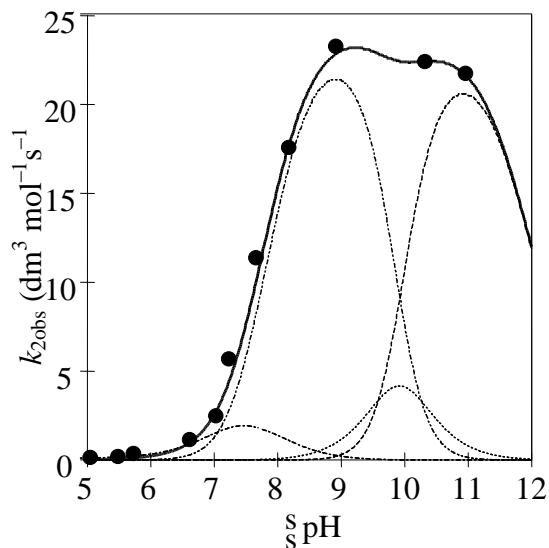


Figure 3. Plot of the predicted k_2^{obs} vs. ^spH rate profile for La^{3+} -catalyzed methanolysis of paraoxon **2** (solid line) based on the kinetics contributions of (left to right), $\text{La}^{3+}_2(\text{OCH}_3)_1$, $\text{La}^{3+}_2(\text{OCH}_3)_2$, $\text{La}^{3+}_2(\text{OCH}_3)_3$, and $\text{La}^{3+}_2(\text{OCH}_3)_4$ computed from the $k_2^{2:1}$, $k_2^{2:2}$, $k_2^{2:3}$, and $k_2^{2:4}$ rate constants (Table 1) and their speciation as a function of ^spH .
(Reproduced with permission from Gibson et al.²³)

When the kinetics and speciation data are fitted to eq 1, individual second-order rate constants for each of the $(\text{La}^{3+})_2(\text{OCH}_3)_n$ species ($k_2^{2:n}$) can be determined. These are presented in Table 1.

$$k_2^{\text{obs}} = \{k_2^{2:1}[\text{La}^{3+}_2(\text{OR})_1] + k_2^{2:2}[\text{La}^{3+}_2(\text{OR})_2] + k_2^{2:n}[\text{La}^{3+}_2(\text{OR})_n]\} / [\text{La}(\text{OTf})_3]_t \quad (1)$$

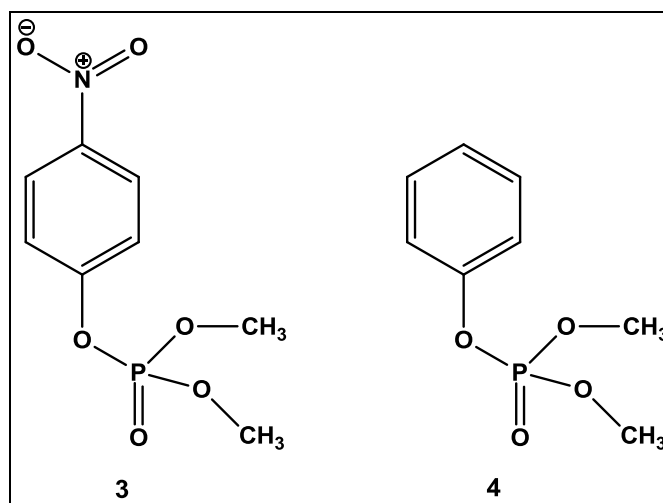
Table 1. Computed Second-Order Rate Constants ($k_2^{2:n}$) for the $(\text{La}^{3+})_2(\text{OCH}_3)_n$ -Catalyzed Methanolysis of Paraoxon **2** Obtained through Fits of k_2^{obs} at Each s pH to Eq 1

$(\text{La}^{3+})_2(\text{OCH}_3)_n$ Species	$k_2^{2:n}$ ($\text{dm}^3 \text{ mol}^{-1} \text{ s}^{-1}$)
OCH_3^-	$k_{\text{OCH}_3} = 0.011$
$(\text{La}^{3+})_2(\text{OCH}_3)_1$	$k_2^{2:1} = 15.8 \pm 2.9$
$(\text{La}^{3+})_2(\text{OCH}_3)_2$	$k_2^{2:2} = 51.1 \pm 1.1$
$(\text{La}^{3+})_2(\text{OCH}_3)_3$	$k_2^{2:3} = 35.6 \pm 6.5$
$(\text{La}^{3+})_2(\text{OCH}_3)_4$	$k_2^{2:4} = 49.7 \pm 1.4$

Notes:

- (1) Errors were computed from average percent deviations in fitted numbers calculated by eq 1 from actual kinetics data.
- (2) Data in part from Tsang et al. (high s pH)²² and Gibson et al.²³

The activation parameters presented in Table 2 were determined for the OCH_3^- - and La^{3+} -catalyzed methanolysis of methyl paraoxon **3** and its parent compound, dimethyl phenyl phosphate **4**. Although the enthalpies and entropies of activation for the base-catalyzed processes are as expected for this type of the reaction, the La^{3+} -catalyzed processes have unusually low activation parameters. Those values are consistent with the mechanism that proceeds through the formation of a transient complex between the catalyst and the substrate, followed by an “intramolecular” delivery of the metal ion-coordinated nucleophile to a substrate that is activated by Lewis acid coordination to the La^{3+} center(s). In such a case, the overall enthalpy of activation can be separated into two parts, the first arising from the interaction between the catalyst and the substrate and the second relating to the actual “chemical” step. The expected negative value of the first component partially compensates the expected small, but positive, enthalpy of activation characteristic of an intramolecular Lewis acid-promoted nucleophilic attack, which results in an overall enthalpy close to zero in the case of methyl paraoxon **3**. In the case of the slightly less electrophilic parent ester **4**, the second part should have a slightly higher positive enthalpy of activation, consistent with the values given in Table 2. The low change in enthalpy (ΔH^\ddagger) resulting from the complex-promoted cleavage of the bound substrates is achieved at the price of a large negative entropy, as would be expected for a highly ordered transition state involving association of two species with severely restricted degrees of freedom. Nevertheless, the low ΔH^\ddagger value means that the reactions are not very temperature dependent: reducing the temperature from 25 to -25 °C will only reduce the reaction rate by factors of 1.27 and 3 for substrates **3** and **4**, respectively.



Structure **3**. Dimethyl *p*-nitrophenyl phosphate.

Structure **4**. Dimethyl phenyl phosphate.

Table 2. Activation Parameters for the Base- and La^{3+} -Catalyzed Methanolysis of Dimethyl *p*-Nitrophenyl Phosphate (**3**) and Dimethyl Phenyl Phosphate (**4**)

Substrate	Term	Catalyst	
		CH_3O^-	$(\text{La}^{3+})_2$
3	ΔH^\ddagger (kJ mol $^{-1}$)	61.6	3.14
	ΔS^\ddagger (J K $^{-1}$ mol $^{-1}$)	-67	-194.7
	ΔG^\ddagger (25 °C) (kJ mol $^{-1}$)	81.7	61.1
	ΔH^\ddagger (kJ mol $^{-1}$)	65.3	13.8
4	ΔS^\ddagger (J K $^{-1}$ mol $^{-1}$)	-72.9	-183
	ΔG^\ddagger (25 °C) (kJ mol $^{-1}$)	87	72.4

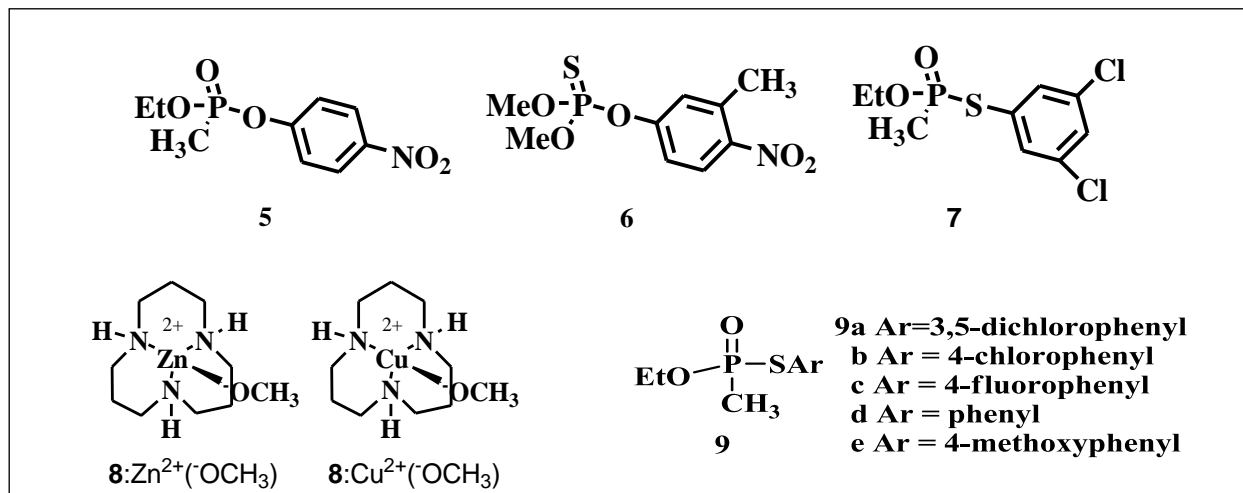
ΔS^\ddagger , change in entropy

ΔG^\ddagger , change in Gibbs free energy

4. METHANOLYSIS OF PHOSPHOROTHIOATES, PHOSPHONATES, AND PHOSPHONOTHIOATES

We have also investigated the metal ion-promoted methanolysis of other OP compounds such as ethyl aryl methylphosphonate (**5**),²⁴ dimethyl aryl phosphorothioate (**6**),²⁵ and ethyl aryl methylphosphonothioate (**7**)²⁶ in the presence of La^{3+} , $\mathbf{8}:\text{Zn}^{2+}(\text{OCH}_3)$, and $\mathbf{8}:\text{Cu}^{2+}(\text{OCH}_3)$. The reactions were studied at $s\text{pH}$ values that would generate the maximum rates for the metal-catalyzed reaction, which generally result when the complexes are formulated with one equivalent of methoxide for each metal ion present. For La^{3+} , the reaction $s\text{pH}$ was set at 9.1 using *N*-ethylmorpholine buffer in which the dominant species was $(\text{La}^{3+})_2(\text{OCH}_3)_2$, while for $\mathbf{8}:\text{Zn}^{2+}(\text{OCH}_3)$ and $\mathbf{8}:\text{Cu}^{2+}(\text{OCH}_3)$, the operational $s\text{pH}$ was set through half-neutralization of the complexes at 9.3 and 8.75,²⁷ respectively. The second-order rate constants (k_2 values) for the $(\text{La}^{3+})_2(\text{OCH}_3)_2$ -catalyzed reactions once again were defined as the slopes of the plots of the pseudo-first-order rate constants (k_{obs}) versus the catalyst concentrations. In the case of the $\mathbf{8}:\text{Zn}^{2+}(\text{OCH}_3)$ and $\mathbf{8}:\text{Cu}^{2+}(\text{OCH}_3)$ reactions, the k_2 values were twice the values of the gradients

of these plots because setting the s pH by half-neutralization of the complexes produces only half of the active species. Based on those values, we calculated the expected $t_{1/2}$ values for the methanolysis of various substrates catalyzed by 1 mmol dm⁻¹ of the active complex at 25 °C (Table 3).



Structure **5**. Ethyl aryl methylphosphonate.

Structure **6**. Dimethyl aryl phosphorothioate.

Structure **7**. Ethyl aryl methylphosphonothioate.

Structure **8**. Zn²⁺(⁻OCH₃) and Cu²⁺(⁻OCH₃) complex.

Structure **9**. S-aryl methylphosphonothioates.

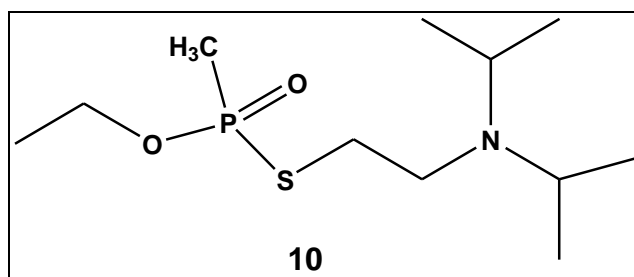
Table 3. Expected $t_{1/2}$ Times for the Methanolysis of Organophosphates **5**, **6**, and **7** Catalyzed by a 1 mmol dm⁻³ Solution of Various Metal Ion Complexes at 25 °C

Catalyst	$t_{1/2}$ (s)		
	5	6	7
La ³⁺ ₂ (⁻ OCH ₃) ₂	0.55	NR	0.14
8 :Cu ²⁺ (⁻ OCH ₃)	2.9	58	—
8 :Zn ²⁺ (⁻ OCH ₃)	15	1027	7.4

NR, no reaction

—, data not available

To predict the reactivity of metal complexes toward the actual U.S. V agent (**10**), we prepared a series of substituted S-aryl methylphosphonothioates (**9a–e**) as simulants that structurally resemble this agent. In Figure 4 are presented three Brønsted plots of log k_2^{catalyst} versus s pK_a (the negative logarithm of the equilibrium constant for association) of aryl thiol for the methanolysis of the series **9a–e** catalyzed by (La³⁺)₂(⁻OCH₃), **8**:Zn²⁺(⁻OCH₃), and methoxide anion, where the respective slopes of the linear plots are $\beta = -0.75 \pm 0.01$, $\beta = -0.66 \pm 0.04$, and $\beta = -0.65 \pm 0.10$.



Structure **10**. U.S. VX (USVX): *O*-ethyl-*S*-(2-diisopropylaminoethyl) methylphosphonothioate (CAS no. 50782-69-4).

We independently determined a ${}^s\text{p}K_a$ of 9.54 for ionization of the SH group of (*N,N*-diethylamino)ethanethiol (a thiol that resembles the leaving group of VX) in methanol. When placed on the various Brønsted plots, this ${}^s\text{p}K_a$ value yields predicted second-order rate constants for the reaction of VX promoted by the three nucleophiles. Accordingly, 1 mmol dm⁻³ solutions of **8**:Zn²⁺(⁻OCH₃) or (La³⁺)₂(⁻OCH₃)₂ are predicted to decompose VX with half-times of 18 and 0.33 s.¹⁶

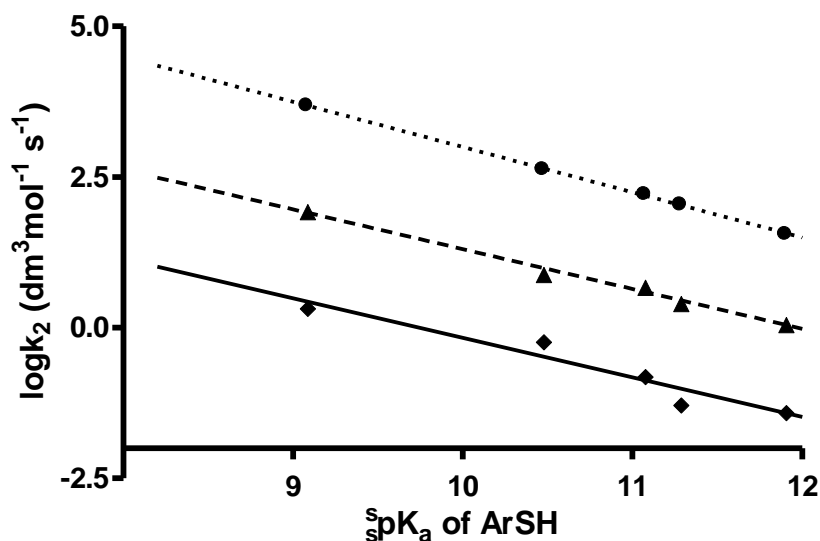


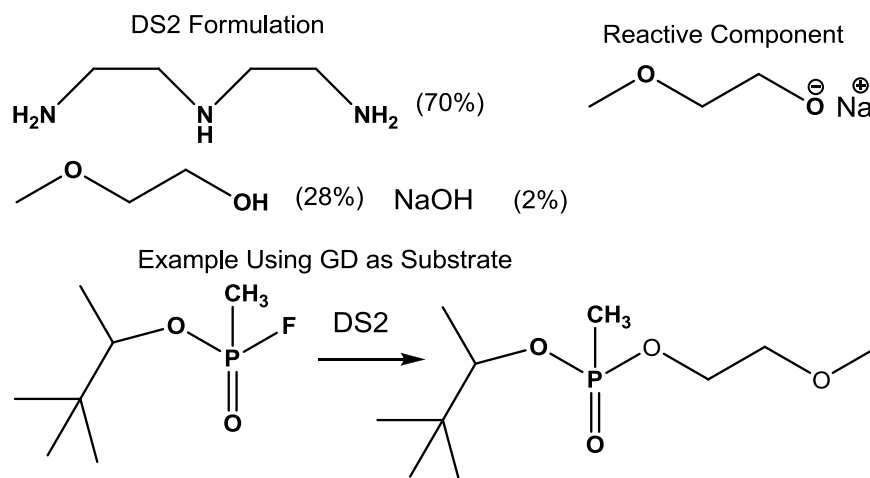
Figure 4. Brønsted plots for $\log k_2^{\text{catalyst}}$ versus ${}^s\text{p}K_a$ of aryl thiol with (La³⁺(⁻OCH₃))₂ (●), **4**:Zn²⁺(⁻OCH₃) (▲), and ⁻OCH₃ (◆). (Reproduced with permission from Melnychuk et al.²⁶)

5. TRANSESTERIFICATION IN CWA DECONTAMINATION: BACKGROUND

Although not widely recognized, the use of transesterification as a basis for destruction of CWAs has a rich history. A brief summary is provided for review.

5.1 Decontamination Solution 2 (DS2)

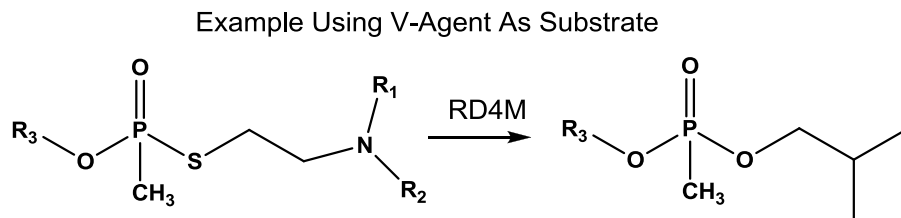
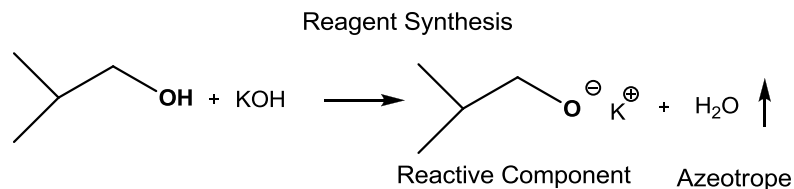
This organic solution, fielded by the U.S. Army in the early 1960s, consists of 2-methoxyethanol (methyl cellosolve; CAS no. 109-86-4), diethylenetriamine (CAS no. 111-40-0), and sodium hydroxide (CAS no. 1310-73-2) in a ratio of 28/70/2 wt %. Although initially thought to be a very effective hydroxide base solution, mechanistic studies by Leslie et al.^{28,29} in the mid-1980s demonstrated that hydroxide reacts with 2-methoxyethanol to produce the alkoxide form of this alcohol, and that with phosphorus-based CWAs, this is the nucleophile responsible for the chemistry. This solution is also deactivated by the addition of water such that the reaction must be as organic as possible for the chemistry to be effective. This solution has low capacity, and it is stoichiometric, very caustic, and fast. This sequence is represented by the following reactions:



5.2 Russian Reactive Decontaminant 4, Modified (RD4M)

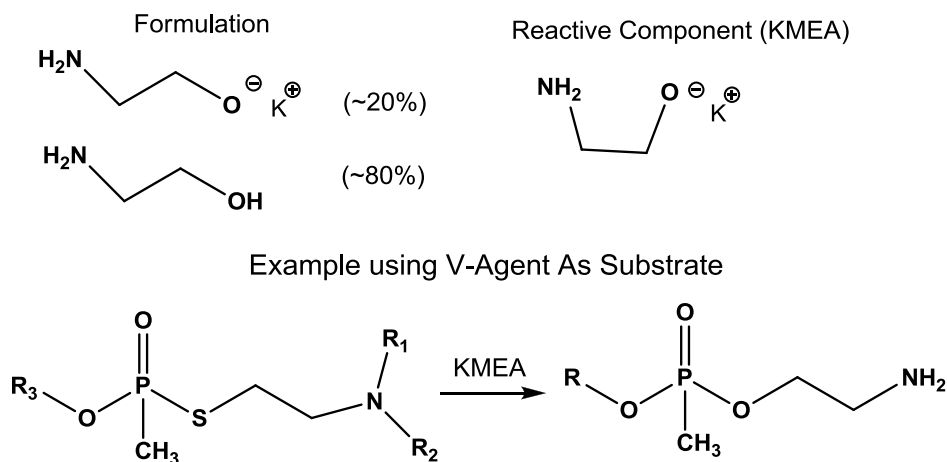
In 1994 and 1995, the chemistry of RD4M was extensively studied through the Russian–American Joint Evaluation Program (RAJEP)^{30–32} in Edgewood, MD and in Seratov, Seratov Oblast, Russian Federation. The solution essentially consists of potassium isobutylate in isobutyl alcohol. This reagent was demonstrated to be effective against GD and RVX, with the mechanism being transesterification at phosphorus. Although it is expensive and dangerous to make by classical synthetic methods (using potassium metal and anhydrous isobutanol), RD4M was effectively produced by a proprietary process developed by the State Research Institute of Organic Chemistry and Technology (GosNIIOKhT; Moscow, Russia) using potassium hydroxide as the source of base. After demonstration of the chemistry from the RAJEP program, this reagent was approved for use in the Russian CW demilitarization program. This solution has

high capacity, and it is stoichiometric, very caustic, and fast. This sequence is represented in the following reactions:



5.3 Mono-Ethanolamine: U.S. Non-Stockpile Decontamination Solution

In 1997, based on experience gained with the RD4M system, ECBC personnel developed a reagent that comprised mono-ethanolamine (CAS no. 141-43-5) and potassium hydroxide (CAS no. 1310-58-3).³³⁻³⁷ This solution was effective against V-type compounds. Mechanistic studies indicated that, like DS2, the active component in the mixture was the alkoxide, not the hydroxide, of mono-ethanolamine. This solution had very high capacity and was caustic, fast, and stoichiometric. This chemistry is represented by the following:



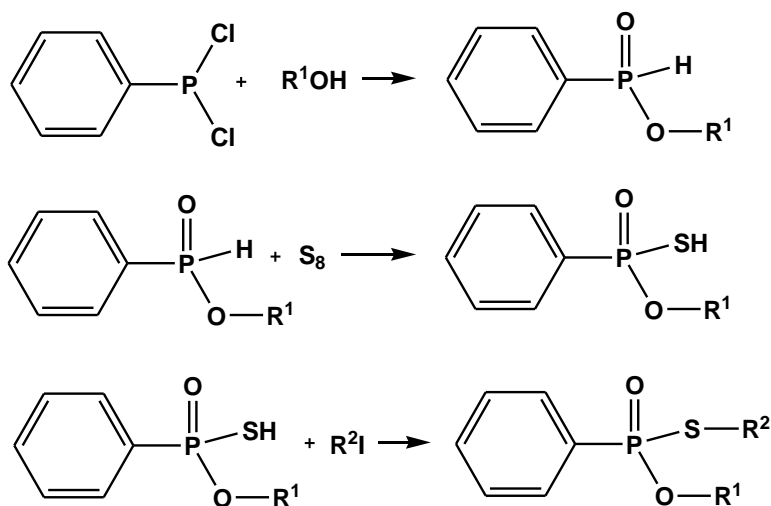
5.4 DS2, RD4M, and Mono-Ethanolamine: Advantages and Disadvantages

In all three examples, the reaction kinetics are very fast and the production of EA 2192 is suppressed (unlike the chemistry associated with aqueous hydroxide- or bleach-based systems). All of these, however, are caustic (DS2 being a particularly corrosive solution) and stoichiometric. Material compatibility is a significant issue with the use of these systems.

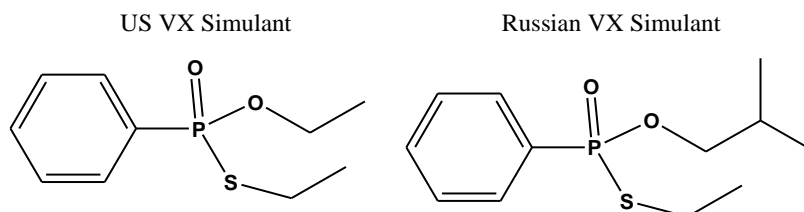
6. EXPERIMENTAL METHODS

6.1 Simulant for G Agents Developed

We have used an effective simulant for V agents developed by Dr. Fred Berg (ECBC) that yields good correlation between V agents in range-finding studies. Based on inexpensive starting materials (*P,P*-dichlorophenylphosphine; D71984, Sigma-Aldrich; St. Louis, MO), a general synthesis based on the work of DeBruin et al.³⁸ is outlined in this scheme:



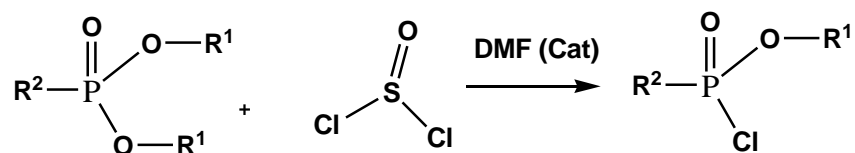
This general synthesis was used to prepare the USVX simulant (*O*-ethyl-*S*-ethylphenylphosphonate, CAS no. 57557-80-9) and the RVX simulant (*O*-isobutyl-*S*-ethylphenylphosphonate, CAS no. not assigned), as shown:



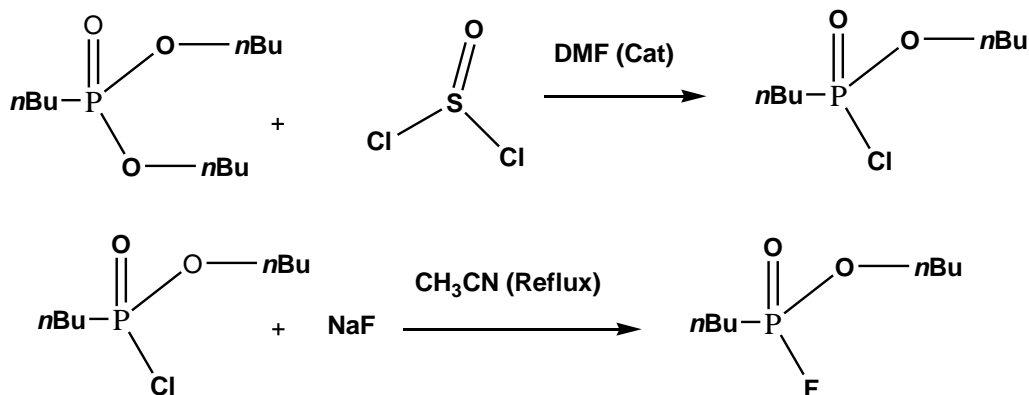
Examination of the literature was performed to determine the toxicity of the USVX simulant and whether exposure to this material leads to OP ester-induced delayed neuropathy (OPIDN or delayed neurotoxicity). OPIDN is characterized by flaccid paralysis of the extremities accompanied by axonal degeneration. OPIDN can occur after a single exposure

or multiple-dose exposures to OP compounds having the structure-activity requirements necessary to generate the delayed neurotoxicity. In experiments to study the delayed neurotoxicity of the USVX simulant in hens, no OPIDN symptoms were exhibited.³⁹ In additional studies of this class of compounds, no delayed neurotoxic effects were indicated.⁴⁰ Based on these results, this class of simulants are not considered delayed neurotoxicants. In the acute toxicity data for this compound,⁴¹ the oral dose that is lethal to 50% of test subjects (the LD₅₀ value) is 75 mg/kg for rats, which is considered only mildly toxic. This contrasts with the methylphosphonic acid equivalent ester, *O,S*-diethyl methylphosphonothioate (CAS no. 2511-10-6; EA 5533), for which an oral LD₅₀ of 3.7 mg/kg for rats was determined.⁴² This class of compounds has been documented in several studies as simulants for V-type agents.⁴³⁻⁴⁷ A similar compound for G agents has not been described.

Chemistry has been developed starting with diester alkylphosphonate, which when reacted with thionyl chloride (CAS no. 7719-09-7) in the presence of a catalytic amount of dimethylformamide (DMF; CAS no. 68-12-2) leads to the production of the mono-ester phosphonochloridate:



Application of this chemistry to di-*n*-butyl-*n*-butylphosphonate (CAS no. 78-46-6; commercially available from Sigma-Aldrich, catalog no. 512427) cleanly gives *n*-butyl-*n*-butylphosphonochloridate (CAS no. 54176-90-8). By application of chemistry developed here at ECBC, a simple reaction of properly prepared NaF converts the chloro-compound into the G analog *n*-butyl-*n*-butylphosphonoflouridate (CAS no. not assigned) in high yields using a simple synthetic workup. These transformations are as follows:

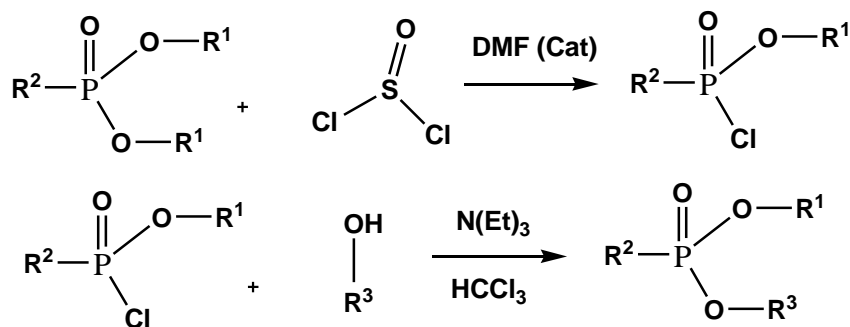


To our knowledge, this derivative of the G class has not been reported in the open literature.

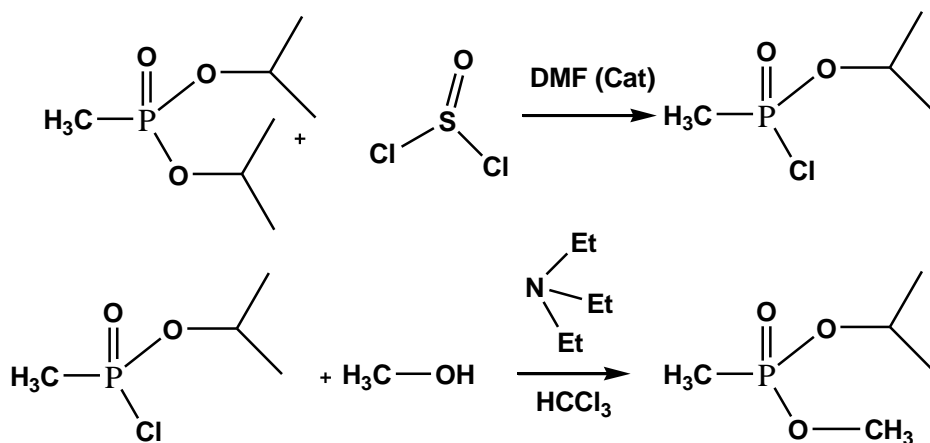
The advantages of both simulants are that (1) they are not controlled by the treaty, nor defined as surety agents by the Army; (2) they require inexpensive, commercially available reagents; and (3) the toxicity of alkylphosphonofluoridates, where the alkyl group is not methyl, ethyl, propyl, or isopropyl, is much lower than those with that structure. The reaction and physical properties chemistries are very close to those of GF/GD agents. Toxicology testing is being planned, and results will be included in a separate technical report.

6.2 Synthesis of Product Standards

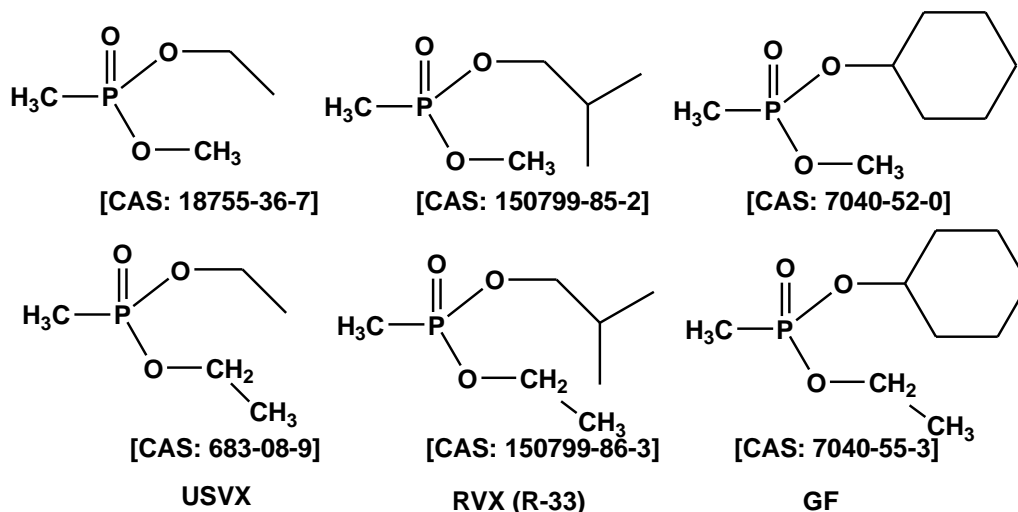
During evaluation of the different variations of solvent systems, a standard procedure for synthesis of the expected products was developed. At the core of the strategy was the use of the thionyl chloride reaction (shown above) for the synthesis of the G agent simulant. The synthesis diverges at the chloridate stage, where instead of conversion to the fluoride derivative, conversion to the mixed ester is accomplished. This strategy begins with relatively inexpensive, commercially available starting materials and allows multiple product variations to be obtained with essentially the same synthetic procedure, which is outlined as



A specific example of this general transformation is the conversion of diisopropyl methylphosphonate (DIMP; CAS no. 1445-75-6) into methyl isopropyl methylphosphonate through the intermediate chloridate, which is the expected product from GB (sarin), as shown:

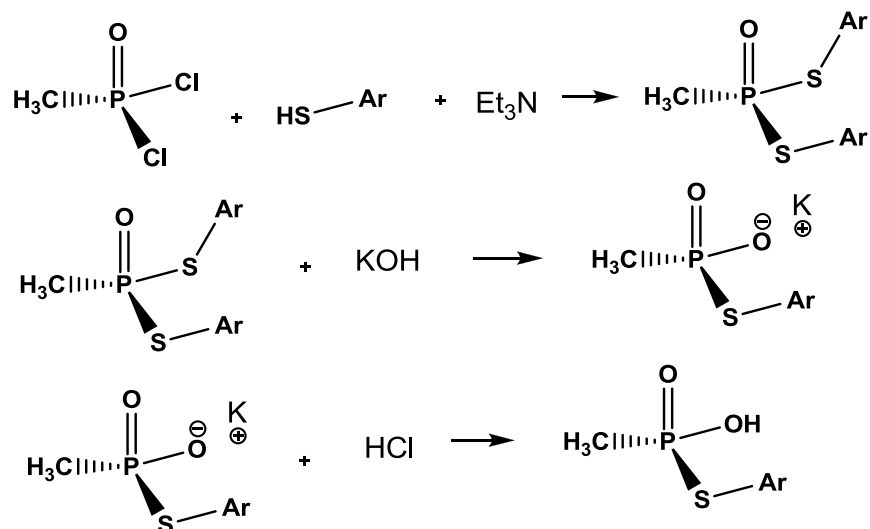


The products obtained from USVX, RVX (R-33), and GF using System 4/5 in methanol and ethanol are presented below:



6.3 Synthesis of Model EA 2192 Compounds

All anionic phosphonothioates (**11a–e**) were prepared by the following general route from methylphosphonic dichloride via *S,S'*-diarylmethylphosphonothioate. Thiophenol (10 mM) was added to a solution of methylphosphonic dichloride (5 mM) in dry dichloromethane and triethylamine (10 mM) was slowly added to the mixture. The reaction mixture was stirred at 40 °C for 4 h. After removal of the solvent under reduced pressure, the residue was dissolved in 15 mL dichloromethane. The dichloromethane solution was washed with water (6 × 15 mL), and the combined aqueous layers were extracted with dichloromethane (3 × 15 mL). The combined organic layers were washed with saturated aqueous sodium chloride (10 mL) and dried over anhydrous sodium sulfate, and the isolated product was *S,S'*-diarylmethylphosphonothioate (90% yield). The *S,S'*-diarylmethylphosphonothioate solution was then added to a mixture of 5 M aqueous potassium hydroxide (3 mL) and dioxane (16 mL) and stirred at 50 °C for 8 h. The solution was concentrated under reduced pressure to remove dioxane. To remove the thiol from the aqueous layer, the pH was brought down to 6–7 and the thiol was extracted with dichloromethane. The aqueous layer was then acidified with 3 M aqueous hydrogen chloride (20 mL), and the acidic solution was extracted with dichloromethane (3 × 15 mL). The combined extracts were washed with saturated aqueous sodium chloride (10 mL) and dried over anhydrous sodium sulfate. Dichloromethane was removed under reduced pressure, and the isolated product was pure acid phosphonothioate (≥80% yield). The reaction sequence is outlined as follows:



6.4 Ethanolamine/La³⁺-Mediated Decomposition of Phosphonate Substrates

6.4.1 Materials

Ethanolamine (purified grade) was purchased from Fisher Scientific (Pittsburg, PA). Lanthanum trifluoromethanesulfonate (La(OTf)₃), tetrabutylammonium fluoride ((Bu₄N⁺)F⁻), and samarium trifluoromethanesulfonate (Sm(OTf)₃) were purchased from Sigma-Aldrich. Lanthanum methanesulfonate (La(OMs)₃) was purchased from Chemical and Technical Developments Ltd. (Salisbury, Wilts, U.K.).

6.4.2 Kinetics Study

Stock solutions of 50 mM La(OTf)₃, La(Ms)₃, and Sm(OTf)₃ were prepared in ethanolamine. Sodium ethoxide (50 mM) was prepared in anhydrous ethanol. A stock solution of 150 mM (Bu₄N⁺)F⁻ was prepared in ethanolamine. Stock solutions (10 mM) of *p*-nitrophenyl ethyl methylphosphonate and paraoxon were prepared in acetonitrile. Kinetics studies were performed by UV-vis spectrophotometry, and the kinetics of appearance of the *p*-nitrophenoxide product was monitored at 25 °C and 385 nm under pseudo-first-order conditions of excess catalyst. In each experiment, the final volume was 2.5 mL.

In the first set of kinetics experiments, 1, 2, 3, and 5 mM solutions of La(OTf)₃ or La(Ms)₃ in ethanolamine were prepared, and *p*-nitrophenyl ethyl methylphosphonate was added to achieve a final concentration of 0.02 mM. Results are shown in Table 5.

To study the effects of cosolvents, solutions of 1, 2, 3, and 5 mM La(X)₃ (where X = OTf, OMs) were prepared in 70% ethanolamine with either 30% ethanol (v/v) or 30% methanol (v/v), and the kinetics of decomposition of *p*-nitrophenyl ethyl methylphosphonate were monitored. Results are shown in Tables 6 and 7.

The effects of water and fluoride were studied using 5 mM La(OTf)₃ in ethanolamine, in ethanolamine with 30% ethanol, and in ethanolamine with 30% methanol, and the kinetics of decomposition of *p*-nitrophenyl ethyl methylphosphonate were monitored. Results are shown in Tables 8 and 9.

The effects of water on the decomposition of *p*-nitrophenyl ethyl methylphosphonate were studied using 5 mM Sm(OTf)₃ in ethanolamine and in ethanolamine with 30% methanol. Results are shown in Table 10.

The effects of complex aging on La(OTf)₃ and Sm(OTf)₃ (5 mM) with 20% water present for periods up to 24 h was studied by measuring the rate constant for the reaction with *p*-nitrophenyl ethyl methylphosphonate after 0 min to 24 h of aging in ethanolamine and in ethanolamine with 30% ethanol. Results are shown in Tables 11 and 12.

The behavior of solutions containing high concentrations of La(OTf)₃ (100, 50, and 30 mM) and Sm(OTf)₃ (50 mM) in ethanolamine and in ethanolamine with 30% ethanol was assessed by measuring their effects on the rate constant for decomposition of both paraoxon and *p*-nitrophenyl ethyl methylphosphonate in the presence of variable amounts of water. Results are shown in Tables 13–16.

6.5 CWA Experimental Design

6.5.1 Reaction Criteria

There are two standard, generally recognized criteria for testing the destruction efficiency of reagents upon CWAs. The first is the NATO standard, in which the ratio of agent-to-decontamination sample load is set at 1 to 100 (v/v). The second is that common in U.S. testing, whereby the agent-to-decontamination sample load is set at 1 to 50 (v/v). In addition, an in-house addition to the 1/50 ratio is used at ECBC, such that the minimum rate for destruction kinetics should be 10 half-lives in 10 min at room temperature.

6.5.2 “Force-to-Fail” Criteria

In addition to the common reaction criteria as discussed in the preceding paragraph, another set of criteria, called force to fail, was developed at ECBC in the mid-1980s. The experimental sequence in force to fail starts as a “load-load” agent-to-decontamination solution (1/100; 1/50). The agent load is increased in separate multiple additions, and the reaction progress is monitored. The chemistry shuts down at the force-to-fail point, and significant quantities of residual agent remain after addition.

6.5.3 Experimental Design

Virtually all of the evaluations at ECBC were performed using ³¹P-NMR techniques on a JEOL ECX-400 spectrometer operating at 161.83 MHz fitted with an ASC8 Auto Sample Changer (JEOL; Peabody, MA). All measurements were performed at 22 °C.

Baseline resonance frequencies for neat agent in methanol were measured before every series at the 2.5% load. To evaluate force to-fail-criteria at low neat-agent concentrations (less than ~8%), neat agent was measured into an NMR tube, and a set volume of decontamination reagent was added to the tube. The sample was mixed by shaking and then immediately positioned in the ASC8 Auto Sample Changer for entry into the spectrometer. The total time elapsed between mixing and first results was ~4 min. Continued interrogation of the sample was performed every 2 min until either no agent peak was observed or the 10 min time limit had been reached. To evaluate force-to-fail criteria at higher neat-agent concentrations (greater than ~8%), the neat agent was first weighed into a 4 mL vial. In a separate 4 mL vial, the appropriate decontamination solution was measured. The decontamination solution was added to the agent vial, and the contents were mixed before being added to an NMR tube. NMR measurements were performed as for the low-concentration evaluations.

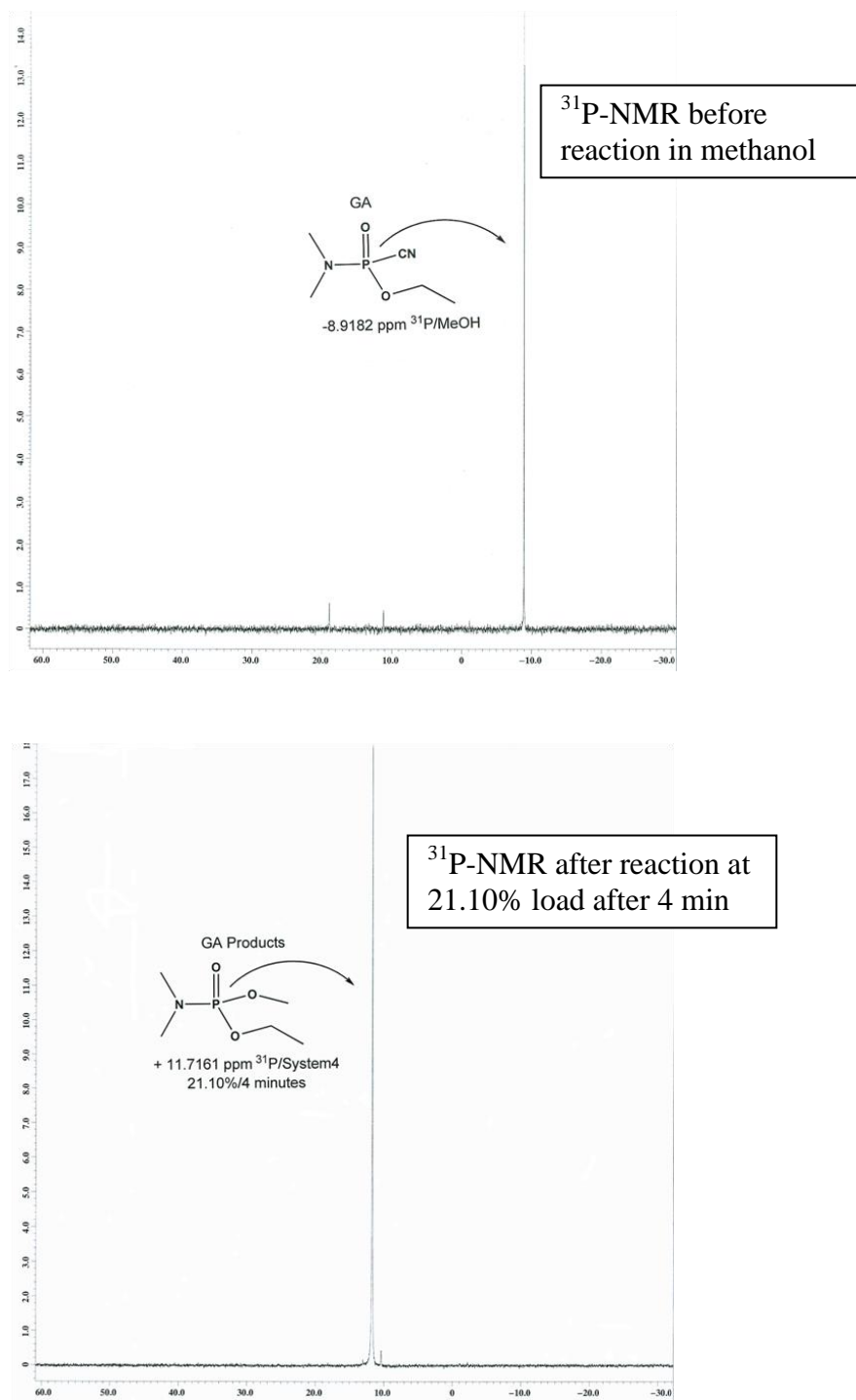
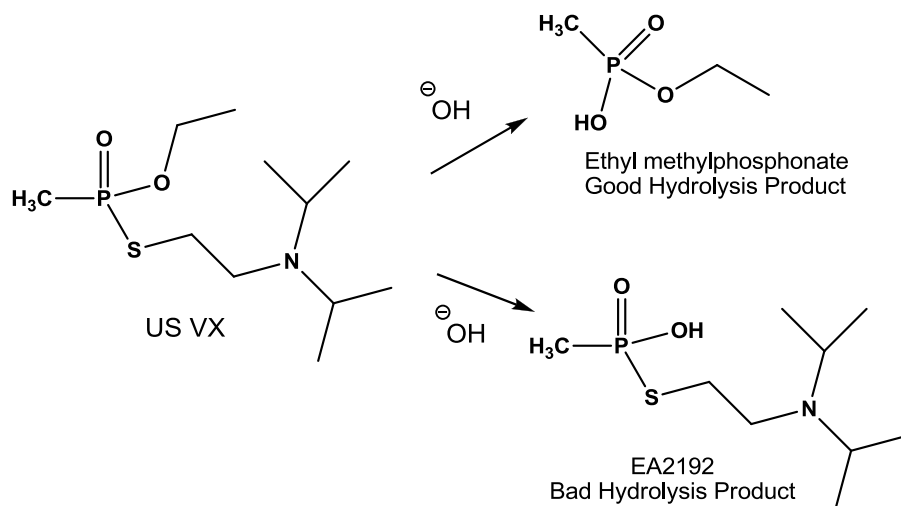


Figure 5. Data example: GA reaction using System 4 (S4) from Queen's University.

7. RESULTS

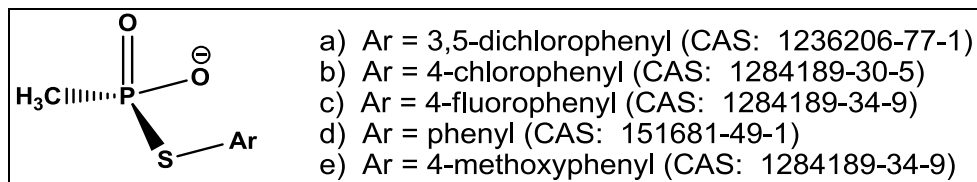
7.1 Hydrolysis versus Transesterification: The EA 2192 Problem

MICA (System 4) is a lanthanide/methanol-based decontamination solution that exhibits extremely high activity for the decomposition of organophosphorous CWAs such as G and V agents. However, samples of V agents, particularly ones subjected to weathering, can contain products of partial V agent hydrolysis, namely, EA 2192 (**1**) (${}^-\text{OP}(\text{CH}_3)(=\text{O})(\text{SR})$). Also, EA 2192 can be formed during decontamination procedures that include hydrolytic methodologies.



At room temperature, EA 2192 is a white solid. It is infinitely soluble and extremely stable in water at neutral and alkaline pHs. It is more stable to hydrolysis than VX: in a solution of 0.1 N NaOH and at a temperature of 25 °C, no significant hydrolysis occurred within 12 days. The carbon partition coefficient ($\log K_{\text{OC}}$) of EA 2192 is 1.90, which indicates a low potential to adsorb to soil. The octanol/water partition coefficient ($\log K_{\text{OW}}$), however, is 0.96, which indicates small bioconcentration factors for aquatic life.

We have prepared a series of model compounds^{48,49} for EA 2192 that are based on methyl phosphonic acid with a variety of leaving groups (**11a–e**).



Structure **11**. Model EA 2192 compounds with various leaving groups.

Preliminary kinetics studies were performed of the decomposition of EA 2192 model compounds **11a–e** using lanthanum triflate solutions in the range of 1×10^{-4} to 2.5×10^{-3} M. The pH was controlled using various noninhibitory buffers, including *N*-methylimidazole (s pH of 7.60), *N*-ethylmorpholine (s pH of 8.28), and triethylamine (s pH of 10.78) buffers, which were partially neutralized with triflic acid. Reaction progress was monitored using UV-vis spectroscopy.

Plots of k_{obs} versus $[\text{La}^{3+}]_t$ data for methanolysis of **11** are somewhat unusual, particularly at low pH values. At s pH of 8.4–8.7, the catalytic effect of $[\text{La}^{3+}]_t$ changes rapidly to attenuation of the catalysis with further increase in La^{3+} concentration. In the example presented in Figure 6 (s pH of 8.4), k_{obs} decreased from 5×10^{-4} M $< [\text{La}^{3+}] < 1.5 \times 10^{-3}$, then remained almost constant with increasing $[\text{La}^{3+}]_t$. In the case of high s pH values (Figure 2; s pH of 11.7), the rate constant increased with $[\text{La}^{3+}]_t$, and then saturation phenomena were observed.

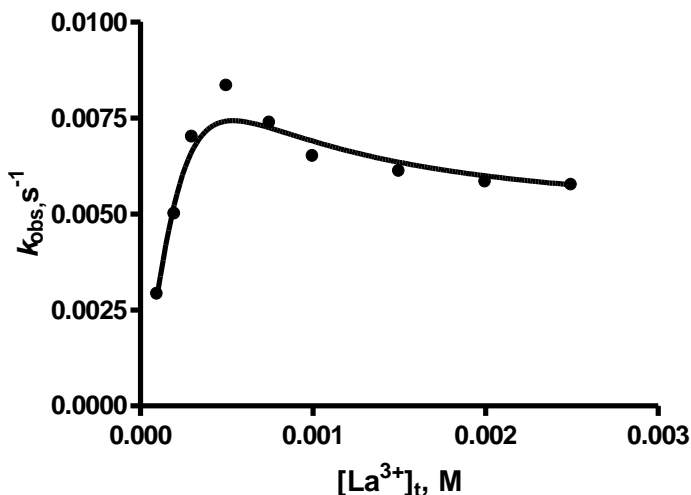


Figure 6. Plot of pseudo-first-order rate constant for the methanolysis of **11a** (1×10^{-4} M) versus $[\text{La}(\text{OTf})_3]$ at 25.0 ± 0.1 °C and a s pH of 8.4 (in 0.04 M *N*-ethylmorpholine buffer).

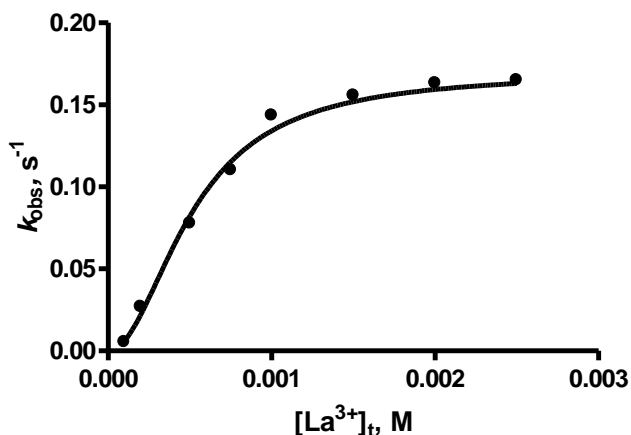


Figure 7. Plot of pseudo-first-order rate constant for the methanolysis of **11a** (1×10^{-4} M) versus $[\text{La}(\text{OTf})_3]$ at 25.0 ± 0.1 °C and a s pH of 11.7 (in 0.04 M triethylamine buffer).

Experimental data from the plots of k_{obs} versus $[\text{La}^{3+}]_t$ data for methanolysis of **11** were analyzed in terms of the second-order rate constant for the reaction of **11** with $\text{La}^{3+}(\text{CH}_3\text{O}^-)_m (k_1)$ and pseudo-first-order rate constant for methanolysis of complex $(\text{La}^{3+})_2\text{:2:}(\text{CH}_3\text{O}^-)_n (k_{\text{cat}})$. Representative data for compound **11b** at various ^spH values are provided in Table 1.

Table 4. ^spH Dependence of the Second-Order Rate Constant for the Reaction of **11b** with $\text{La}^{3+}(\text{CH}_3\text{O}^-)_m (k_1)$ and Pseudo-First-Order Rate Constant for Methanolysis of $(\text{La}^{3+})_2\text{:2:}(\text{CH}_3\text{O}^-)_n (k_{\text{cat}})$ at 25.0 ± 0.1 °C

^spH	$k_1 (\text{M}^{-1} \text{s}^{-1})$	$10^3 k_{\text{cat}} (\text{s}^{-1})$
7.6	3.40 ± 0.30	0.32
8.4	5.96 ± 0.60	0.58
8.9	8.75 ± 0.62	3.33
9.9	15.0 ± 1.2	7.33
10.9	10.8 ± 1.0	12.16
11.7	5.85 ± 0.40	18.33

7.2 Effect of Leaving Group on Reactivity of Model Compounds **11** and Prediction of EA 2192 Reactivity

Figure 8 shows the Brønsted plots of $\log k_{\text{cat}}$ versus experimentally determined $^s\text{p}K_{\text{a}}^{\text{HSAr}}$ values for the corresponding thiophenols for the La^{3+} -promoted cleavage of **11a–e** at ^spH 8.4 and 11.7. In both cases, the plots are straight lines described by eqs 2 and 3:

$$\log k_{\text{cat}}^{8.4} = (4.02 \pm 0.36) - (0.69 \pm 0.03) ^s\text{p}K_{\text{a}}^{\text{HSAr}} \quad r^2 = 0.99 \quad (2)$$

$$\log k_{\text{cat}}^{11.7} = (3.79 \pm 0.35) - (0.52 \pm 0.03) ^s\text{p}K_{\text{a}}^{\text{HSAr}} \quad r^2 = 0.99 \quad (3)$$

$$\log k_{\text{cat}}^{\text{System4}} = (4.22 \pm 0.33) - (0.72 \pm 0.03) ^s\text{p}K_{\text{a}}^{\text{HSAr}} \quad r^2 = 0.99 \quad (4)$$

From our previous report of La^{3+} -promoted methanolysis of VX analogues, the predicted value of $^s\text{p}K_{\text{a}}$ for $\text{HSCH}_2\text{CH}_2\text{N}(\text{CH}(\text{CH}_3)_2)_2$ was ~ 9.54 . Therefore, the predicted k_{cat} values computed from eqs 2 and 3 for EA 2192 were 2.74×10^{-3} and $6.75 \times 10^{-2} \text{ s}^{-1}$ at ^spH values of 8.4 and 11.9, respectively.

To provide a better forecast of the EA 2192 decomposition rate using the MICA solution (System 4), we have studied the decomposition rates of the **11a–e** series of model compounds in MICA solution (System 4). The data presented in Figure 8 and the Brønsted correlation in eq. 4 indicate that the rate of decomposition of model compounds in MICA solution (System 4) is closely correlated with the pseudo-first-order rate constant for methanolysis of $(\text{La}^{3+})_2\text{:Sub:}(\text{CH}_3\text{O}^-)_n (k_{\text{cat}})$.

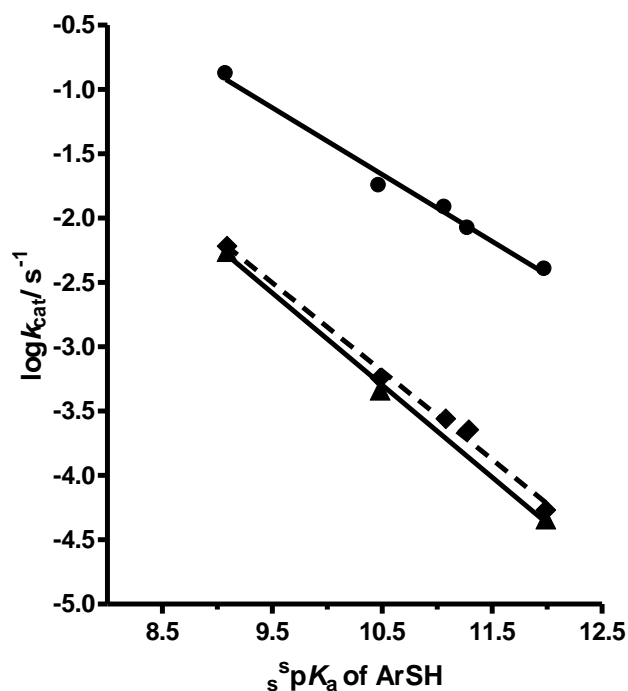


Figure 8. Brønsted plots for the La^{3+} -catalyzed methanolysis of EA 2192 analogues **11** (solid line) determined at $s \text{ pH}$ of 11.7 and temperature of 25.0 ± 0.1 °C, where $\log k_{\text{cat}}^{8.4} = (4.02 \pm 0.36) - (0.69 \pm 0.03)s \text{ p}K_a^{\text{HSAr}}$, $r^2 = 0.99$; and (dashed line) determined at $s \text{ pH}$ of 8.4 and temperature of 25.0 ± 0.1 °C, where $\log k_{\text{cat}}^{8.4} = (3.79 \pm 0.35) - (0.52 \pm 0.03)s \text{ p}K_a^{\text{HSAr}}$, $r^2 = 0.99$. Solid, \blacktriangle line indicates $\log k_{\text{cat}}$ versus $s \text{ p}K_a^{\text{HSAr}}$ for the reactions between **11a–e** and MICA (System 4), where $\log k_{\text{cat}}^{\text{System4}} = (4.22 \pm 0.33) - (0.72 \pm 0.03)s \text{ p}K_a^{\text{HSAr}}$, $r^2 = 0.99$.

7.3 Results for Ethanolamine/ La^{3+} -Mediated Decomposition of Phosphonate Substrates

Table 5. Concentration Dependence of Various La-Based Catalysts in EA toward Solvolysis of *p*-Nitrophenyl Ethyl Methylphosphonate (0.02 mM) at 25 °C

$[\text{La}]/k_{\text{obs}}$ (min^{-1})	$\text{La}(\text{OTf})_3$	$\text{La}(\text{Ms})_3$
1 mM	2.69	2.96
2 mM	4.44	4.55
3 mM	6.93	7.10
5 mM	10.30	11.65

Table 6. Concentration Dependence of Various La-Based Catalysts in EA/Ethanol Mixture (70/30% v/v) toward Solvolysis of *p*-Nitrophenyl Ethyl Methylphosphonate (0.02 mM) at 25 °C

$[La]/k_{obs}$ (min ⁻¹)	La(OTf) ₃	La(Ms) ₃
1 mM	2.69	2.34
2 mM	4.41	3.86
3 mM	8.18	6.41
5 mM	12.35	11.07

Table 7. Concentration Dependence of Various La-Based Catalysts in EA/Methanol Mixture (70/30% v/v) toward Solvolysis of *p*-Nitrophenyl Ethyl Methylphosphonate (0.02 mM) at 25 °C

$[La]/k_{obs}$ (min ⁻¹)	La(OTf) ₃	La(Ms) ₃
1 mM	2.03	2.83
2 mM	3.46	4.82
3 mM	9.48	7.05
5 mM	22.51	15.53

Table 8. Effect of Extraneous Water Added to the 5 mM Solution of La(OTf)₃ in EA, EA/Ethanol Mixture (70/30% v/v), and EA/Methanol Mixture (70/30% v/v) on the Solvolysis Rate of *p*-Nitrophenyl Ethyl Methylphosphonate (0.02 mM) at 25 °C

%H ₂ O/ k_{obs} (min ⁻¹)	EA + 30% Ethanol	EA + 30% Methanol	EA
0%	12.35	22.51	10.30
1%	6.08	8.32	5.53
2%	3.87	5.20	4.26
5%	2.60	2.68	3.91
10%	1.07	1.88	1.86
20%	0.57	1.06	1.47

Table 9. Effects of Fluoride Anion Addition to the 5 mM La(OTf)₃ Solution in EA, EA/Ethanol Mixture (70/30% v/v), and EA/Methanol Mixture (70/30% v/v) on the Solvolysis Rate of *p*-Nitrophenyl Ethyl Methylphosphonate (0.02 mM) at 25 °C

$[F^-]/k_{obs}$ (min ⁻¹)	EA+ 30% Ethanol	EA+ 30% Methanol	EA
0 mM	12.35	22.51	10.30
5 mM	7.51	8.05	5.84
10 mM	3.43	2.89	1.91
20 mM	0.79	0.78	1.14

Table 10. Effects of Extraneous Water Added to the 5 mM Sm(OTf)₃ Solution in EA and EA/Ethanol Mixture (70/30% v/v) on the Solvolysis Rate of *p*-Nitrophenyl Ethyl Methylphosphonate (0.02 mM) at 25 °C

%H ₂ O/ <i>k</i> _{obs} (min ⁻¹)	EA+ 30% Methanol	EA
0%	13.67	6.58
1%	11.56	6.42
2%	12.75	5.62
5%	3.96	5.37
10%	1.93	2.79

Table 11. Effects of La(OTf)₃ Aging in the Presence of 20% (v/v) Water on the Rate Constant for Reaction with *p*-Nitrophenyl Ethyl Methylphosphonate in EA and EA/Ethanol Mixture (70/30% v/v) at 25 °C

Time of Aging (min)/ <i>k</i> _{obs} (min ⁻¹)	EA	70% EA+ 30% Ethanol
0	1.41	0.70
30	1.29	0.52
60	1.01	0.41
120	0.94	0.50
180	0.91	0.36
1440	0.87	0.24

Table 12. Effects of Sm(OTf)₃ Aging in the Presence of 20% (v/v) Water on the Rate Constant for Reaction with *p*-Nitrophenyl Ethyl Methylphosphonate in EA and EA/Ethanol Mixture (70/30% v/v) at 25 °C

Time of Aging (min)/ <i>k</i> _{obs} (min ⁻¹)	EA	70% EA+ 30% Ethanol
0	1.18	0.52
30	0.81	0.43
60	0.84	0.31
120	0.80	0.37
180	0.82	0.30
1440	0.74	0.33

Table 13. Effects of Extraneous Water Added to the 100 mM La(OTf)₃ Solution in EA and EA/Ethanol Mixture (70/30% v/v) on the Paraoxon (0.02 mM) Solvolysis Rate at 25 °C

H ₂ O%/ <i>k</i> _{obs} (min ⁻¹)	EA	EA+ 30% Ethanol
0	34.67	25.30
1	13.59	5.23
2.5	4.01	1.50
5	1.16	0.87
10	0.64	0.24
15	0.38	

Table 14. Effects of Extraneous Water Added to the 50 mM La(OTf)₃ Solution in EA and EA/Ethanol Mixture (70/30% v/v) on the Paraoxon (0.02 mM) Solvolysis Rate at 25 °C

H ₂ O%/k _{obs} (min ⁻¹)	EA	EA+ 30% Ethanol
0	24.91	14.21
1	4.87	2.92
2.5	1.29	0.40
5	0.38	0.42
10	0.27	0.13
15	0.24	
20	0.15	
30	0.15	

Table 15. Effects of Extraneous Water Added to the 30 mM La(OTf)₃ Solution in EA and EA/Ethanol Mixture (70%/30% v/v) on the Paraoxon (0.02 mM) Solvolysis Rate at 25 °C

H ₂ O%/k _{obs} (min ⁻¹)	EA	EA+ 30% Ethanol
0	12.8	13.0
1	2.8	1.3
2.5	0.51	0.21
5	0.19	0.14
10	0.15	0.13

Table 16. Effects of Extraneous Water Added to the 50 mM Sm(OTf)₃ Solution in EA and EA/Ethanol Mixture (70%/30% v/v) on the Paraoxon (0.02 mM) Solvolysis Rate at 25 °C

H ₂ O%/k _{obs} (min ⁻¹)	EA	EA+ 30% Ethanol
0	6.85	3.73
1	4.09	1.61
2.5	2.44	0.98
5	1.45	0.73
10	0.57	0.28

7.4 Destruction of CWAs Using Force-to-Fail Criteria

Based on the experimental designed described in Section 6.5, several catalytic systems in methanol, ethanol, and mono-ethanolamine, containing La³⁺, Sm³⁺, buffer, and other ingredients, were formulated and tested at ECBC. These were evaluated for their efficacy in decomposing OP CWAs, namely GA, GB, GD, GF, USVX (Chemical Agent Standard Analytical Reference Material [CASARM]), USVX (Munition), RVX (CASARM), and RV-bis. Results are summarized in Table 17.

Table 17. Catalytic Systems Formulated and Tested for Efficacy in Decomposing OP CWAs

Agent ^a	Decontamination System	Load at Force to Fail (%)
GA (tabun)	S4 (La ³⁺ /methanol)	>29.50
GB (sarin)	S4 (La ³⁺ /methanol)	2.50
GD (soman)	S4 (La ³⁺ /methanol)	2.50
GF (cyclosarin)	S4 (La ³⁺ /methanol)	2.50
GF (cyclosarin)	S5 (Sm ³⁺ /methanol)	6.00
GF (cyclosarin)	E4 (La ³⁺ /ethanol)	3.90
GF (cyclosarin)	E5 (Sm ³⁺ /ethanol)	6.70
USVX (CASARM)	S4 (La ³⁺ /methanol)	24.90
USVX (munitions)	S4 (La ³⁺ /methanol)	~15
RVX (CASARM)	S4 (La ³⁺ /methanol)	20.00
USVX (CASARM)	S4a (La ³⁺ /methanol)	34.00
USVX (Munitions)	S4a (La ³⁺ /methanol)	33.70
USVX (CASARM)	E4 (La ³⁺ /methanol)	19.20
RVX (CASARM)	E4 (La ³⁺ /methanol)	23.90
GF (cyclosarin) ^b	S12 (La ³⁺ /MEA)	>8.00
USVX (CASARM)	S12 (La ³⁺ /MEA)	17.20
USVX (CASARM)	S14 (Sm ³⁺ /MEA)	5.36
RV-bis ^c	S4 (La ³⁺ /methanol)	21.20

^a All agents are CASARMs with at least 95% purity.

^b G agents, such as GF, react exothermically with MEA. Because of the heat produced, the force-to-fail experiment in this case did not proceed beyond the 8.00% indicated;

^c RV-bis (CAS no. 92030-06-3; phosphorodithioic acid; methyl-S,S-bis[diethylamino]ethyl ester), is a component of munitions-grade RVX. It is reported to be as toxic as RVX itself.

7.5 TNO Agent Results

Independent, contract laboratory testing at the Netherlands Organisation for Applied Scientific Research (TNO) in Rijswijk, The Netherlands was also performed on the solution S4 (La³⁺/methanol). The activities for GA, GD, USVX, and sulfur mustard (HD) were studied at a 50:1 (v:v) challenge (50 parts of System 4 decontaminant solution, 1 part CWA). Analyses were performed and reaction products were obtained by NMR or gas chromatography–mass spectrometry (GC-MS), and, in the case of VX, also by liquid chromatography–mass spectrometry (LC-MS). Given the predicted high efficiency of the decontamination method, all samples were analyzed as quickly as possible after the addition of all components. This involved quenching the reaction by addition of HCl to the decontaminating solution that contained the agent, and was followed by NMR analysis. System 4 was also tested on solid surfaces, namely, panels coated with chemical agent-resistant coating (CARC). Panels were coated with 10 g/m² CWA, and after a 10 min decontamination time, the reactions were stopped, and residual agent was solvent-extracted and analyzed by GC-MS.

In the 50:1 challenge-liquid solution tests, all of the OP agents (GA, GD, and VX) were destroyed in less than 30 s (the minimal possible testing time), and no residual nerve agents were detected in solution by GC-MS at a detection limit of <200 ng/mL. After completion of each reaction, only the nontoxic corresponding *O*-methylation product was identified for each

nerve agent. Notably, it was shown that the possible toxic degradation product of VX, EA 2192 (an often-found product of decontamination in aqueous solution), was not formed during the decomposition of USVX (at a detection limit of <1 ppm).

The solution also decontaminated nerve agents on CARC panels (at a loading of 10 g/m²) within 10 min using a minimal amount of the solution (<1 mL/cm²) with no scrubbing or agitation. The efficiency of the decontamination was >99%, and in most cases, >99.9% (Table 18). In the case of HD, although the solution removed 95% of the material from the CARC panel within 10 min, the blister agent was not destroyed but was simply removed through its solubility in methanol. This suggests that System 4 might have practical use for HD removal from surfaces; however, the recovered solution would still contain active material that requires post-treatment.

Table. 18. Decontamination Efficiency of Decontamination System against GA, GD, VX, and HD on CARC Panels

Agent (10 g/m ²)	Reaction Time (min)	Decontamination Efficiency (%) ^a
GA	10	>99.9
GD		99.2
VX		>99.9
HD		95

^a Detection limit, 0.5 µg/cm³. Amount corrected for extraction efficiencies.

7.6 Agent Testing at Research Institute of Hygiene, Occupational Pathology, and Human Ecology (RIHOPHE)

Further testing of System 4 was performed in the spring of 2009 in collaboration with Queen's University (Ontario, Canada) and RIHOPHE (St. Petersburg, Russia). The testing involved a 50:1 challenge of RVX (20 mg/mL or 20,000 ppm), and analysis of the reaction mixture was performed using direct-injection GC-MS techniques. These tests established that after 1 min, no residual RVX was present in the solution (at a detection limit of <1 ppm), which indicated that >99.995% decontamination had occurred within that time.

8. DISCUSSION

8.1 Destruction Efficiency of System 4

A summary of the force-to-fail agent results described in the preceding sections clearly show that System 4 (La³⁺/methanol) was extremely efficient at transesterification decomposition of nonfluoride agents (GA and V class): agent loads of 15–35% were generated using the designated reaction criteria. Because of interaction and inhibition of fluoride with the La³⁺ metal ion, the G class agents were decomposed at higher efficiencies than the 1:50 ratio, but

those results were not nearly as impressive as the results for non-fluoride-releasing agents. Lanthanide ions are highly Lewis acidic; therefore, their interactions with fluoride anions are very strong and inhibitory. This inhibition effect was ameliorated by Sm^{3+} substitution as the metallic ion catalysis progressed (at loads of ~6–7%). Attempts to use other strategies to address this fluoride ion issue have yet to yield effective solutions for obtaining loads comparable with those obtained for the GA and V class agents.

8.2 Alternative Solvents

System 4 is a lanthanide/methanol-based decontamination solution that exhibits extremely high activity for decomposition of OP CWAs (such as G and V agents). However, many issues must be addressed. One is the perceived toxicity and flammability of the methanol-based solution. A possible solution (improvement) is the use of ethanol as the main component in the decontamination system. Ethanol is generally considered to be far less toxic than other alcohols, and it has a higher flash point than methanol, which should (to a certain degree) mitigate flammability issues. As indicated by the summary of agent results (Table 17), substitution of ethanol for methanol (as in Systems E4 and E5) does not significantly affect the destruction efficiency. For example, comparison of the two ethanol-based formulations of Systems E4 and E5 with the methanol formulation of System S4 at the 5% load factor with RVX showed that within the first time point during the NMR experiment (~3.5 min), all three provided baseline VX destruction (peak at ~58 ppm destroyed, and ester peaks at 31–33 ppm as only phosphorus peaks). Force-to-fail experiments above the 5% load with both USVX and RVX yielded comparable loads as those observed in System 4 experiments. Continued experimentation with mono-ethanol amine clearly indicated that this solvent can be substituted for both methanol and ethanol. Recent work also indicated that mixtures of all three alcohols were effective as supporting solvents for this chemistry. Thus the flash point of the solvent can be adjusted over a large range and “tuned” to the application.

8.3 Effects of Water on Reactivity

A few examples of full-strength decontamination solutions were created, and in all cases, they had very high reactivities for the decomposition of the CW model compound, paraoxon. The ability to withstand the inhibitory effects of extraneous moisture was tested, and it was demonstrated that a samarium-based catalytic system had the best resistance to extraneous moisture. This is important for any “real-life” scenario. These results will allow us to formulate a metal ion-based catalytic system for decomposition of live OP CWAs that is suitable for any given application and proceed to testing on “live” agents.

8.4 Simulant Reactivity

Two non-agent simulants for V agents, *O*-ethyl-*S*-ethyl methylphosphonate and *O*-ethyl-*S*-ethyl phenylphosphonate, were tested at the 5% load to the solutions above. All were degraded in a very similar manner to V agents, although at a somewhat slower rate. This observation provides nonclassified laboratories with an acceptable simulant for V agents, so that data related to the mechanism of transesterification can be obtained before the expense of agent testing is initiated. Testing of the G agent simulant directly against GF is scheduled for future work.

8.5 Production and Decomposition of EA 2192

There is no evidence that EA 2192 was produced in any of the solvent combinations reported upon herein. Preliminary results indicated that Systems S4 (La^{3+} /methanol) and S12 (La^{3+} /MEA) appeared to slowly decompose EA 2192. Exact kinetics results have not yet been obtained, and future work will address this result.

8.6 Low-Level Residual Agent Concentration

In the force-to-fail experimental design, the use of ^{31}P -NMR limited the detection limit of residual agents to approximately 0.1–0.05%. The exact residual agent concentration was not part of the original ECBC analytical protocol. Results from TNO and RIHOPHE that were obtained using GC-MS and LC-MS systems indicated considerably greater destruction efficiency. Thus, at the end of the project period of performance, the adaption of two new techniques was in progress: a liquid chromatography–tandem mass spectroscopy technique based on the work of E. Michael Jakubowski (ECBC)⁵⁰ and an enzyme-inhibition assay based on the procedure reported by RIHOPHE.⁵¹ Future evaluation of this chemistry will include an attempt to use these procedures to better understand low-level residual agent concentrations.

9. CONCLUSIONS

Metal ion-catalyzed methanolysis provides a simple yet effective methodology for the decontamination of neutral OPs of the phosphate, phosphonate, phosphorothioate, and phosphonothioate classes. The most effective catalysts to date for alcoholysis of the compounds containing the $\text{P}=\text{O}$ unit are those containing lanthanide ions, particularly La^{3+} , and certain complexes of transition metal ions, notably Zn^{2+} and Cu^{2+} , at near-neutral pH values. A system containing La^{3+} buffered at a pH of 9 (System 4) has also been shown to catalyze the decontamination of OP chemical weapons, including GA, GB, GD, and other G agents, as well as USVX and RVX, producing nontoxic products by methanolysis. On the other hand, La^{3+} -based catalysts were ineffective for the decomposition of neutral OP materials that contain $\text{P}=\text{S}$, some of which have uses as pesticides.

LITERATURE CITED

1. United States Chemical Weapons Convention website;
http://www.cwc.gov/cwc_treaty.html (accessed June 2013).
2. Morales-Rojas, H.; Moss, R.A. Phosphorolytic Reactivity of *o*-Iodosylcarboxylates and Related Nucleophiles. *Chem. Rev.* **2002**, *102*, pp 2497–2521.
3. Pearson, G.S.; Magee, R.S. Critical Evaluation of Proven Chemical Weapon Destruction Technologies (IUPAC Technical Report). *Pure Appl. Chem.* **2002**, *74*, pp 187–316.
4. Yang, Y.C.; Baker, J.A.; Ward, J.R. Decontamination of Chemical Warfare Agents. *Chem. Rev.* **1992**, *92*, pp 1729–1743.
5. Yang, Y.C. Chemical Detoxification of Nerve Agent VX. *Acc. Chem. Res.* **1999**, *32*, pp 109–115.
6. Yang, Y.C. Chemical Reactions for Neutralizing Chemical Warfare Agents. *Chem. Ind. (London)* **1995**, *9*, pp 334–337.
7. Brown, R.S.; Neverov, A.A. Acyl and Phosphoryl Transfer to Methanol Promoted by Metal Ions. *J. Chem. Soc. Perkin Trans. 2*, **2002**, p. 1039
8. Brown, R.S.; Neverov, A.A.; Tsang, J.S.W.; Gibson, G.T.T.; Montoya-Pelaez, P.J. 2004 Bader Award Lecture Metal-Ion-Catalyzed Acyl and Phosphoryl Transfer Reactions to Alcohols: La³⁺-Promoted Alcoholysis of Activated Amides, Carboxylate Esters, and Neutral Organophosphorus Esters. *Can. J. Chem.* **2004**, *82*, pp 1791–1805.
9. Brown, R.S.; Neverov, A.A. *Advances in Physical Organic Chemistry*; Richard, J.P., Ed.; Vol. 42; Elsevier: San Diego, CA, 2007, p 271.
10. Yang, H.; Carr, P.D.; McLoughlin, S.; Yu, L.J.W.; Horne, I.; Qiu, X.; Jeffries, C.M.J.; Russell, R.J.; Oakeshott, J.G.; Ollis, D.L. Evolution of an Organophosphate-Degrading Enzyme: A Comparison of Natural and Directed Evolution. *Protein Eng.* **2003**, *16*, pp 135–145.
11. Jackson, C.J.; Foo, J.-L.; Kim, H.-K.; Carr, P.D.; Liu, J.-W.; Salem, G.; Ollis, D.L. In Crystallo Capture of a Michaelis Complex and Product-Binding Modes of a Bacterial Phosphotriesterase. *J. Mol. Biol.* **2008**, *375*, pp 1189–1196.
12. Kim, J.; Tsai, P.-C.; Chen, S.-L.; Himo, F.; Almo, S.C.; Raushel, F.M. Structure of Diethyl Phosphate Bound to the Binuclear Metal Center of Phosphotriesterase. *Biochemistry* **2008**, *47*, pp 9497–9504.
13. Lipscomb, W.N.; Straeter, N. Recent Advances in Zinc Enzymology. *Chem. Rev.* **1996**, *96*, pp 2375–2434.
14. Coleman, J.E. Zinc Enzymes. *Curr. Opin. Chem. Biol.* **1998**, *2*, pp 222–234.

15. Cowan, J.A. Metal Activation of Enzymes in Nucleic Acid Biochemistry. *Chem. Rev.* **1998**, 98, pp 1067–1088.
16. Davies, J.F.; Hostomska, Z.; Hostomsky, Z.; Jordan, S.R.; Matthews, D.A. Crystal Structure of the Ribonuclease H Domain of HIV-1 Reverse Transcriptase. *Science* **1991**, 252, pp 8–95.
17. Beese, L.S.; Steitz, T.A. Structural Basis for the 3'-5' Exonuclease Activity of *Escherichia coli* DNA Polymerase I: A Two Metal Ion Mechanism. *EMBO J.* **1991**, 10, pp 25–33.
18. Lahm, A.; Volbeda, A.; Suck, D. Crystallisation and Preliminary Crystallographic Analysis of P1 Nuclease from *Penicillium citrinum*. *J. Mol. Biol.* **1990**, 215, pp 207–210.
19. Gani, D.; Wilkie, J. Stereochemical, Mechanistic, and Structural Features of Enzyme-Catalyzed Phosphate Monoester Hydrolysis. *Chem. Soc. Rev.* **1995**, 24, pp 55–63.
20. Omburo, G.A.; Kuo, J.M.; Mullins, L.S.; Raushel, F.M. Characterization of the Zinc Binding Site of Bacterial Phosphotriesterase. *J. Biol. Chem.* **1992**, 267, pp 13278–13283.
21. Cleland, W.W.; Frey, P.A.; Gerlt, J.A. The Low Barrier Hydrogen Bond in Enzymic Catalysis. *Biol. Chem.* **1998**, 273, pp 25529–25532.
22. Tsang, J.S.; Neverov, A.A.; Brown, R.S. Billion-Fold Acceleration of the Methanolysis of Paraoxon Promoted by La(OTf)₃ in Methanol. *J. Am. Chem. Soc.* **2003**, 125, pp 7602–7607.
23. Gibson, G.; Neverov, A.A.; Brown, R.S. Potentiometric Titration of Metal Ions in Methanol. *Can. J. Chem.* **2003**, 81, pp 495–504.
24. Lewis, R.E.; Neverov, A.A.; Stan Brown, R.S. Mechanistic Studies of La³⁺ and Zn²⁺-Catalyzed Methanolysis of O-ethyl O-aryl Methylphosphonate Esters. An Effective Solvolytic Method for the Catalytic Destruction of Phosphonate CW Simulants. *Org. Biomol. Chem.* **2005**, 3, pp 4082–4088.
25. Desloges, W.; Neverov, A.A.; Brown, R.S. Zn²⁺-Catalyzed Methanolysis of Phosphate Triesters: A Process for Catalytic Degradation of the Organophosphorus Pesticides Paraoxon and Fenitrothion. *Inorg. Chem.* **2004**, 43, pp 6752–6761.
26. Melnychuk, S.A.; Neverov, A.A.; Brown, R.S. Catalytic Decomposition of Simulants for Chemical Warfare V Agents: Highly Efficient Catalysis of the Methanolysis of Phosphonothioate Esters. *Angew. Chem. Int. Ed. Engl.* **2006**, 45, pp 1767–1770.
27. Neverov, A.A.; Brown, R.S. Cu(II)-Mediated Decomposition of Phosphorothioate P=S Pesticides. Billion-Fold Acceleration of the Methanolysis of Fenitrothion Promoted by a Simple Cu(II)-Ligand System. *Org. Biomol. Chem.* **2004**, 2, pp 2245–2248.

28. Beaudry, W.T.; Szafraniec, L.L.; Leslie, R.D. *Reactions of Chemical Warfare Agents with DS-2: Product Identification by NMR. 1. Organophosphorus Compounds*; CRDEC-TR-364; U.S. Army Edgewood Research, Development, and Engineering Center: Aberdeen Proving Ground, MD, 1992; UNCLASSIFIED Report (ADA254284).
29. Yang, Y.-C.; Baker, J.A.; Ward, J.R. Decontamination of Chemical Warfare Agents. *Chem. Rev.* **1992**, 92, pp 1729–1743.
30. Sheluchenko, V.V.; Durst, H.D. *Russian-American Experiments; Annotated Report, Two-Stage Process of Sarin, Soman, and Destruction* (JES054; Contract No. DNA001-95-C-0058; BNI Job No. 22911; Bechtel National, Inc.); prepared for the Defense Nuclear Agency, 1995.
31. Morrissey, K.M.; Brickhouse, M.D.; Raghuveer, K.; Williams, B.R.; and Heykamp, L.S. *Chemical Characterization of Reaction Masses, Bitumenized Reaction Masses, and Distillates Produced During the Russian-American Joint Evaluation Program (RAJEP), Final Comprehensive Report*; EAI Report 56/96/001F; EAI Corporation: Abingdon, MD, May 1996.
32. Brickhouse, M.D.; Rees, M.; O'Connor, R.J.; Durst, H.D. *Nuclear Magnetic Resonance (NMR) Analysis of Chemical Agents and Reaction Masses Produced by Their Chemical Neutralization*; ERDEC-TR-449; U.S. Army Soldier Biological Chemical Command: Aberdeen Proving Ground, MD, December 1997; UNCLASSIFIED Report.
33. McGarvey, D.J.; Durst, H.D.; Creasy, W.R.; Ruth, J.L.; Morrissey, K.M.; Stuff, J.R. *Chemical Analysis and Reaction Kinetics of EA-2192 in Decontamination Solution for the MMD-1 Project*; ECBC-TR-282; U.S. Army Soldier Biological Chemical Command: Aberdeen Proving Ground, MD, May 2003; UNCLASSIFIED Report.
34. Morrissey, K.M.; Williams, B.R.; Cheicante, R.; Stuff, J.R.; Durst, H.D. *Quantitative and Qualitative Gas Chromatographic Analysis of Reaction Masses Produced from Chemical Neutralization of GB with Monoethanolamine*; ECBC-TR-041; U.S. Army Soldier Biological Chemical Command: Aberdeen Proving Ground, MD, July 1999; UNCLASSIFIED Report.
35. Morrissey, K.M.; Williams, B.R.; Ruth, J.L.; Stuff, J.R.; Durst, H.D. *Quantitative and Qualitative Gas Chromatographic Analysis of Reaction Masses Produced from Chemical Neutralization of VX with Monoethanolamine*; ECBC-TR-042; U.S. Army Soldier Biological Chemical Command: Aberdeen Proving Ground, MD, July 1999; UNCLASSIFIED Report.
36. *Evaluation of the Chemistry which Supports VX Neutralization in the Munitions Management Device-1 (MMD-1)*; Durst, H.D., Ed.; Comprehensive report prepared for the Project Manager for Non-Stockpile Chemical Materiel; Aberdeen Proving Ground-Edgewood Area, MD, October 1997; UNCLASSIFIED Report.

37. *Evaluation of the Chemistry which Supports GB Neutralization in the Munitions Management Device-1 (MMD-1)*; Durst, H.D., Ed.; Comprehensive report prepared for the Project Manager for Non-Stockpile Chemical Materiel; Aberdeen Proving Ground-Edgewood Area, MD, October 1997; UNCLASSIFIED Report.
38. DeBruin, K.E.; Tang, C.I.W.; Johnson, D.M.; Wilde, R.L. Kinetic Facial Selectivity in Nucleophilic Displacements at Tetracoordinate Phosphorus: Kinetics and Stereochemistry in the Reaction of Sodium Ethoxide with O,S-Dimethyl Phenylphosphonothioate. *J. Am. Chem. Soc.* **1989**, *111*, pp 5871–5879.
39. Hollingshaus, J.G.; Armstrong, D.; Tois, R.F.; McCloud, L.; Fukuto, T.R. Delayed Toxicity and Delayed Neurotoxicity of Phosphonothioate and Phosphonothioate Esters. *J. Toxicol. Environ. Health*, **1981**, *8*, pp 619–627.
40. Hollingshaus, J.G.; Nishioka, T.; March, R.B.; Fukuto, T.R. Effect of Impurities on the Delayed Neurotoxicity of O-(4-bromo-2,5-dichlorophenyl) O-Ethyl Phenylphosphonothioate Administered Orally to Hens. *J. Agric. Food Chem.* **1981**, *29*, pp 593–600.
41. Spector, W.S. *Handbook of Toxicology*; Vol. 1; W.B. Saunders: Philadelphia, PA, 1956, p 4.
42. Wiles, J.S.; Manthei, J.H.; Christesen, M.K. *Toxicological Evaluation in Animals of Simulant Components, Mixtures, and/or Reaction Products for Use in Testing the XM736 8-Inch Binary VX Projectiles*; ARCSL-TR-79501; U.S. Army Chemical Systems Laboratory: Aberdeen Proving Ground, MD, 1980; UNCLASSIFIED Report.
43. Kuo, L.Y.; Adint, T.T.; Akagi, A.E.; Zakharov, L. Degradation of a VX Analogue: First Organometallic Reagent to Promote Phosphonothioate Hydrolysis through Selective P-S Bond Scission. *Organometallics* **2008**, *27*(11), pp 2560–2564.
44. Seabolt, E.E.; Ford, W.T. Alkaline Hydrolysis of O,S-Diethyl Phenylphosphonothioate and p-Nitrophenyl Diethyl Phosphate in Latex Dispersions. *Langmuir* **2003**, *19*(13), pp 5378–5382.
45. Wagner, G.W.; Bartram, P.W. Reactions of VX, HD, and Their Simulants with NaY and AgY Zeolites. *Langmuir* **1999**, *15*(23), pp 8113–8118.
46. Moss, R.A.; Morales-Rojas, H.; Zhang, H.; Park, B.-D. Cleavage of VX Simulants by Micellar Iodoso- and Iodoxybenzoate. *Langmuir* **1999**, *15*(23), pp 8113–8118.
47. Berg, F.J.; Moss, R.A.; Yang, Y.-C.; Zhang, H. Cleavage of Phenylphosphonothioates by Hydroxide Ion and by Micellar Iodosobenzoate. *Langmuir* **1995**, *11*(2), pp 411–413.
48. Dhar, B.B.; Edwards, D.R.; Brown, R.S. A Study of the Kinetics of La³⁺-promoted Methanolysis of S-Aryl Methylphosphonothioates: Possible Methodology for Decontamination of EA 2192, the Toxic Byproduct of VX Hydrolysis. *Inorg. Chem.* **2011**, *50*(7), pp 3071–3077.

49. Andrea, T.; Neverov, A.A.; Brown, R.S. Efficient Methanolytic Cleavage of Phosphate, Phosphonate, and Phosphonothioate Ester Promoted by Solid Supported Lanthanide Ions. *Ind. Eng. Chem. Res.* **2010**, *49*(15), pp 7027–7033.
50. Evans, R.A.; Smith, W.L.; Nguyen, N.P.; Crouse, K.L.; Norman, S.D.; Jakubowski, E.M. Quantification of VX Vapor in Ambient Air by Liquid Chromatography Isotope Dilution Tandem Mass Spectrometric Analysis of Glass Bead Filled Sampling Tubes. *Anal. Chem.* **2011**, *83*(1), pp 1315–1320.
51. Prokofieva, D.S.; Voitenko, N.G.; Gustyleva, L.K.; Babakov, V.N.; Savelieva, E.I.; Jenkins, R.O.; Goncharov, N.V. Microplate Spectroscopic Methods for Determination of the Organophosphate Soman. *J. Environ. Monit.* **2010**, *12*, pp 1349–1354.

Blank

ACRONYMS AND ABBREVIATIONS

CARC	chemical agent-resistant coating
CAS	Chemical Abstract Service
CASARM	Chemical Agent Standard Analytical Reference Material
CW	chemical weapon
CWA	chemical warfare agent
ΔG^\ddagger	change in Gibbs free energy
ΔH^\ddagger	change in enthalpy
ΔS^\ddagger	change in entropy
DMF	dimethylformamide
DS2	decontamination solution 2
GA	tabun (CAS no. 77-81-6)
GB	sarin (CAS no. 107-44-8)
GC-MS	gas chromatography–mass spectrometry
GD	soman (CAS no. 96-64-0)
GF	cyclosarin (CAS no. 329-99-7)
HD	sulfur mustard (CAS no. 505-60-2)
k_{cat}	rate constant
K_{m}	Michaelis constant
k_{obs}	observed first-order rate constant
K_{OC} (log)	carbon partition coefficient
K_{OW} (log)	octanol/water partition coefficient
k_2^{obs}	observed second-order rate constant
$\text{La}(\text{OTf})_3$	lanthanum trifluoromethanesulfonate (CAS no. 52093-26-2)
LC-MS	liquid chromatography–mass spectrometry
LD_{50}	dose that is lethal to 50% of test subjects
$\text{Sm}(\text{OTf})_3$	samarium trifluoromethanesulfonate (CAS no. 52093-28-4)
MEA	monoethanolamine (CAS no. 141-43-5)
MICA	metal ion-catalyzed alcoholysis
OP	organophosphorus
OPIDN	organophosphorus ester-induced delayed neuropathy
$^{\text{s}}\text{pH}$	negative logarithm of the pH in specified solvent
$^{\text{s}}\text{pK}_{\text{a}}$	negative logarithm of the equilibrium constant for association
PTE	phosphotriesterase
RAJEP	Russian–American Joint Evaluation Program
RD4M	Russian reactive decontaminant 4, modified
RV-bis	phosphonodithioic acid; methyl-, <i>S,S</i> -bis[diethylamino ethyl] ester; CAS no. 92030-06-3
RVX	Russian VX, <i>O</i> -(2-methylpropyl)- <i>S</i> -(2-diethylaminoethyl) methylphosphonothioate; CAS no. 159939-87-4
TNO	Netherlands Organisation for Applied Scientific Research
USVX	U.S. VX, <i>O</i> -ethyl- <i>S</i> -(2-diisopropylaminoethyl) methylphosphonothioate; CAS no. 50782-69-4

